Changes in dip and frictional properties of the basal detachment controlling orogenic wedge propagation and frontal collapse: the External central Betics case

A. Jimenez-Bonilla 1), T. Torvela 2), J.C. Balanyá 1), I. Expósito 1), M. Díaz-Azpiroz 1)

1). Departamento de Sistemas Físicos, Químicos y Naturales. Universidad Pablo de Olavide, Sevilla (Spain). Carretera de Utrera km 1, Sevilla, 41013, Spain.

2) University of Leeds, School of Earth and Environment, LS2 9JT, Leeds, UK

Key points

- influence of across-strike changes in the detachment properties and the basement topography on external orogenic wedges
- deformation stages in the Betic fold-and-thrust belt
- Langhian mountain front build-up and subsequent collapse

This article has been accepted for publication and undergone full peer review but has not been through the copyediting, typesetting, pagination and proofreading process which may lead to differences between this version and the Version of Record. Please cite this article as doi: 10.1002/2016TC004196

Abstract

Thin-skinned fold-and-thrust belts (FTBs) have been extensively studied through both field examples and modelling. The overall dynamics of FTBs are, therefore, well understood. One less understood aspect is the combined influence of across-strike changes in the detachment properties and the basement topography on the behaviour of an orogenic wedge. In this paper, we use field data together with reflection seismic interpretation from the External Zones of the Central Betics FTB, S Spain, to identify a significant increase in the wedge basal dip (a basement "threshold") coinciding with the pinch-out of a weak substrate. This induced both changes to the wedge geometry and to the basal friction, which in turn influenced the wedge dynamics. The changing dynamics led to a transient “stagnation” of the FTB propagation, topographic build-up and subsequent collapse of the FTB front. This in turn fed an important Langhian depocenter made up of mass transport deposits. Coevally with the FTB propagation, extension took place both parallel and perpendicular to the orogenic trend. This case study illustrates how across-strike changes in wedge basal properties can control the detailed behaviour of a developing FTB front, but questions remain regarding the time-space interaction and relative importance of the basal parameters.

Keywords: fold-and-thrust belt, basal detachment, mass transport deposit, seismic interpretation, orogenic wedge shape, frictional properties.

1. Introduction.

Fold-and-thrust belts (FTBs; [Poblet and Lisle, 2011]) are one of the most common features accommodating orogenic shortening (e.g. Jura belt, [Burkhard and Sommaruga, 1998], Variscan FTB and the External Zones of the Appalachian Orogen [Woodward, 1987; Gallastegui et al., 1997; Mount, 2014]).

The understanding of FTBs is developed from surface and subsurface data together with analytical, numerical, and analogue modelling, which have successfully simulated their mechanical properties and kinematics. Analogue modelling has been extensively reviewed in Graveleau et al., [2012] with respect to: (1) the classical critical taper theory and its applications [e.g. Davis et al., 1983; Dahlen, 1984; 1990; Suppe, 2007]; (2) models of the effect of frictional vs. plastic substrates [e.g. Liu et al., 1992]; (3) inversion tectonics [e.g. Buchanan and McClay, 1991]; (4) fold vs. fault controlled belts [e.g. Simpson, 2009]; (5) the effect of basal dip [e.g. Koyi and Vendeville, 2003]; and (6) geometries resulting from the accretion of syn-orogenic deposits [e.g. Storti and McClay, 1995]. The vast majority of models assume a planar detachment and uniform detachment mechanical properties and, although a few studies address the influence of changes in either of these [e.g. Calassou et al., 1993; Cotton and Koyi, 2000; Argawal and Argawal, 2002; Bahroudi et al., 2003; Luján et al, 2003; Miyakawa et al., 2010], the interaction of these parameters at a developing thrust front remains unclear. Field studies also show that the interaction of basement topography and substrate properties is complicated but significantly affect the behaviour of the FTB [e.g. Davis and Engelder, 1985; Verges et al., 1992; Krzywiec and Verges, 2007; Fagereng, 2011; von Hagke et al., 2014; this paper].

Foreland and intermontane basins are typically associated with FTBs. Foreland basins form as lithospheric thickening at the orogenic hinterland induces flexure of the

lithosphere [Davis et al., 1983; DeCelles and Giles, 1996; DeCelles, 2012]. Additionally, the continuous evolution of the topography and the slope gradient of the tectonic wedge induce slope breaks at various scales, favouring erosion and/or gravitational collapse and leading to mass transport deposits (MTD). MTD often include the so-called "mélange units" (e.g. in Alps and Apennines; [Burkhard and Sommaruga, 1998; Lucente and Pini, 2008; Festa et al., 2010; Codegone et al., 2012]). In this context, "mélange" are rocks consisting of a plastic matrix wrapping around variably-sized blocks of more competent rocks. Because of the plastic matrix rheology, mélanges commonly act as detachments during later deformation events, when over-run by advancing thrust sheets [e.g. Festa et al., 2010]. Furthermore, mass-wasting itself has been modelled to potentially influence FTB evolution by altering the surface slope angle, overall wedge internal friction, and/or wedge thickness [e.g. Smit et al., 2010].

The main aim of this paper is to study how the time-space evolution of an FTB wedge is influenced by the interaction of wedge-base dip and frictional properties, and how this evolution relates to the initiation of mass wasting and orogen-frontal collapse. We focus on the External Zones of the Central Betics of S Spain (Figs. 1 and 2), where changes in orogenic wedge geometry can be identified by surface and subsurface data. Previous work have established the overall structural features of the area [e.g. Roldán et al., 1988a, b, c, 1992, 2012a, b; Crespo-Blanc, 2007, 2008; Rodríguez-Fernández et al., 2013], but several questions remain concerning the evolving wedge architecture. These include a) the nature and significance of the structural variations along and across the FTB and b) the tectonic significance and origin of the mélange units (the Olistostromic Unit, OU; Fig. 2a). In particular, it is unclear why and how the FTB front seemingly accumulated significant topography during the Langhian (16-14 Ma; see age intervals in Fig. 2b), allowing the erosional and/or extensional dismantling of the FTB front. This is evidenced by the OU

deposition, which requires the presence of a topographic high as source area in this part of the FTB. Using field data and seismic reflection profiles with well data from the central External Zones and the southern part of the Guadalquivir foreland basin (Fig. 1), we address the influence of basement topography and basal detachment properties on the evolution of the FTB, the structural changes and the formation of the OU. Finally, using the critical taper model, we will discuss the relationships between the orogen frontal dismantling, the role of syn-orogenic extensional systems and the FTB front stagnation.

2. Geological Setting

The case study used in this paper comes from the Gibraltar Arc (GA). GA comprises the Betic and Rif chains together with the Alboran basin (Fig. 1). GA formed during the last 25 Ma by the collision of their Internal Zones (upper plate, Alboran domain rocks) against the South Iberian and Maghrebian paleomargins [Vera et al., 2004; Michard et al., 2008]. So-called Flysch Through units, partly deposited on now subducted oceanic lithosphere, are sandwiched between the Alboran domain and the paleomargin units [Durand-Delga et al., 2000]. The GA is broadly divided into the Internal Zones, consisting of the Alboran domain rocks and volcanics, and the External Zones comprising Flyschs Trough units and the paleomargin-derived units (Fig. 1). Most of the Internal Zones are made up by tectono-metamorphic complexes, the lowest being recently interpreted as a subducted South Iberian unit that crops out in a tectonic window [Booth-Rea et al., 2015]. Tectonic stacking in the External Zones was coeval with the extension in the Internal Zones that generated the Alboran Basin [e.g., García-Dueñas et al., 1992; Comas et al., 1999; Platt et al., 2013].

The paleomargin units of the External Zones were deformed in a mainly thin-skinned style during the Miocene [e.g. Balanyá and García-Dueñas, 1987; Crespo-Blanc and Campos, 2001; Luján et al., 2003; 2006; Crespo-Blanc, 2007; Expósito et al., 2012; Platt et al., 2013]. Recent studies on the Betic FTB show that shortening was partially coeval with the development of both arc-parallel and arc-perpendicular extension in the External Zones [e.g. Balanyá et al., 2007, 2012; Azañón et al., 2012; Rodríguez-Fernández et al., 2013; Jiménez-Bonilla et al., 2011, 2012, 2015a, b, 2016]. Erosional processes and gravitational collapse of the orogenic front led to intense reworking of the paleomargin and the Flysch units, forming the so-called "Olistostromic Unit" mélange (OU). OU deposition is dated between Langhian and lower Serravallian (Figs. 2a and b) [Roldán et al., 2012a, b; Rodríguez-Fernández et al., 2013].

In the External Zones, the pre-orogenic sequences deposited onto the Hercynian basement of the South Iberian paleomargin start with Triassic evaporites (mainly gypsum), sandstones and carbonates (Fig. 2b) [Pérez-Valera and Pérez-López, 2003; Pérez-López and Pérez-Valera, 2007]. The overlying Jurassic and Cretaceous marine sequences are shallow-water where deposited on the proximal part of the margin (Prebetics units), while the deeper-shelf and pelagic units of were deposited onto the distal margin (Subbetic units) (Fig. 2) [García-Hernández et al., 1980; Vera et al., 2004]. Only the Subbetic units, thrusted over the Prebetic units, are exposed in the study area (Fig. 2).

The pre-orogenic sequences are unconformably overlain early syn-orogenic Oligocene-Lower Miocene deep-water sediments, followed by the Langhian OU, which is only present along the FTB front (Fig. 2). The youngest units are the para-autochtonous Serravallian-Messinian packages with shallowing-upwards, marine-to-continental sequences are deposited (Fig. 2b) [e.g. Sierro et al., 1996; Roldán et al., 2012a; b; Rodríguez-Fernández et al., 2013].

The main deformation is considered to have progressed into the External Zones of the Central Betics with the stacking and folding of the Subbetic and Prebetic units through the Lower Miocene, although the FTB deformation continued in the NW part of the FTB until Late Miocene. A major detachment developed at the base of the FTB within the Triassic evaporites and mudstones. Above the detachment, the internal stacking of the Subbetic units and their thrusting onto the Prebetics were accommodated by SW-NE to WSW-ENE striking folds and thrusts [Crespo-Blanc et al., 2007; Crespo-Blanc, 2007; 2008; this paper]. After Serravallian times, the orogenic front migrated outward into the Guadalquivir foreland basin [e.g. Maldonado et al., 1997; Medialdea et al., 2004; this paper]. Various studies suggest that this late deformation continued until at least the Messinian, and some areas remain seismically active [e.g. Buforn et al., 1995; Medialdea et al., 2009; Balanyá et al., 2012; Vitale et al., 2014; Jiménez-Bonilla et al., 2015a; Serrano et al., 2015; this paper].

3. Data and Methodology

We analyse 17 commercial multichannel 2D seismic reflection lines, data from 13 wells, and mesoscopic structural data collected through fieldwork in the studied area (Fig. 2a). Modifications to appropriate geological maps and cross-sections [Leyva, 1975; Roldán et al., 1988a, b; c; 1992; Hernáiz et al., 1992; García-Cortés, 1992; Díaz de Neira et al., 1992; Roldán et al., 2012b] have been made through this fieldwork and review of recent publications [Crespo-Blanc, 2007; 2008; Azañón et al., 2012; Rodríguez-Fernández et al., 2013; Roldán et al., 2012a].

The seismic profiles form a grid with > 400 km of total profile length (Fig 3a). Only the most representative profiles and their interpretations are presented in this paper. The well data helped to better constrain the interpretation (Fig. 2a). The seismic lines and well data

were acquired by Exxon, Hispanoil and Chevron between 1950 and 1990, and they are publically available from www.ign.es or http://info.igme.es/infogeof/. The images are also available on the Virtual Seismic Atlas (www.seismicatlas.org). The NW-SE oriented seismic lines are subparallel to the tectonic transport direction, and the NE-SW lines are subparallel to orogenic strike. The grid extends from the inner part of the External Betic FTB to the Guadalquivir basin (GB), but the data are scarcer and of poor quality in the frontal part of the FTB (the FFTB in Fig. 3a).

In the seismic images, both coherent and incoherent seismic noise is substantial. The probable causes are: (1) the low reflectivity and intense deformation of salt and evaporites; (2) abrupt lateral velocity changes (i.e. across thrust planes); (3) diffractions associated with faults and folds; (4) an unknown noise source, probably ground roll, accounting for coherent noise; (5) the lack of coherent reflector structure within the OU, where it has been deposited (mainly in the FFTB and GB) [Roldán et al., 2012a]; and (6) side-swipe (out-of-plane reflections). To help address the noise and artifacts, a seismic facies interpretation method was applied to the seismic profiles [approach of Mitchum and Vail, 1977]. Seismic facies refers to an assemblage of reflections with characteristic parameters (e.g., energy, continuity, dip) and geometrical configurations that can be related to physical changes in the rock. The analysis of seismic facies is a more reliable approach to seismic interpretation than identifying individual (strong) reflections that may result from artefacts such as side-swipe, diffraction, or multiples. In our case, the most identifiable seismic facies coincide with the Jurassic limestones intersected by the well Río Guadalquivir-H1 (Fig. 3a). They are distinguished by their continuous, thick and strongly reflective packages. These form the geometric basis of much of our interpretation. These packages are commonly underlain by noisy packages, usually interpreted as Triassic evaporites. The Tortonian-Messinian sediments of the GB also show good reflectivity, and are underlain by either the chaotic OU

or the Hercynian basement. The interpretations are constrained by surface and well data (Río Guadalquivir H-1 and Río Guadalquivir N-1), where available. Thus, although significant uncertainties remain in the interpretation of structures and due to the poor data quality of some seismic profiles, the elements important for our objectives are identifiable.

The seismic data are displayed in two way travel time (TWT). The maximum penetration is ~4.5 seconds. Assuming an average seismic P-wave velocity of 5300 ms^{-1}, as constrained by well data, is assumed for the Subbetic units [Chourak et al., 2005], this TWT represents c. 12 km depth. The data are, however, commonly too noisy for detailed interpretation below c. 2 s TWT. A velocity of 2500 ms^{-1}, based on well data and Soto et al., [1996], is used for Tortonian to Quaternary sediments within the GB and within the intermontane basins.

The seismic and well data permit the approximation of the main basement topographic features and their slope β [e.g. Dahlen, 1984]. The geometry of the FTB orogenic wedge is obtained by combining β with the surface slope α. The angle α was calculated by a regression analysis of a representative topographic profile with a sampling interval of 1 km.

4. Structure of the Central Betic FTB

Using field data and seismic interpretations, we describe the changes in the structural style of the external Central Betics along a NW-SE cross-section. The studied area is divided into four sectors based on differences in the structural style and the lithostratigraphy of their outcropping units. From SE to NW, they are: the inner fold-and-thrust belt (IFTB), the middle fold-and-thrust belt (MFTB), the frontal fold-and-thrust belt (FFTB) and the Guadalquivir basin (GB).

4.1. Inner fold-and-thrust belt (IFTB)

The IFTB consists of the pre-orogenic Triassic to Palaeogene rocks of the Subbetics, thrusted over the Prebetic units, together with the syn-orogenic, Lower Miocene packages (Figs. 3 and 4). The topographic highs (reaching up to 1570 m) coincide with kilometric-scale anticlines (Figs. 3a, b and 5a), defining fold trains that strike approximately WSW-ENE to SW-NE. The Triassic evaporites commonly crop out in the anticline cores [Crespo-Blanc, 2007; 2008] (Figs. 3a and 4a). Structural features suggest the anticlines are detachment folds: most of them are box-shaped or upright open folds, which often develop high-angle reverse faults along both fold limbs (Figs. 4a, b and c). Folds axial traces generally exceed 10 km and are doubly plunging. Wavelengths are between 2 and 5 km. The axial traces strike N59.5ºE on average (Fig. 4d). The Lower Miocene packages show syn-deformational growth features such as onlaps onto the fold limbs (Figs. 4b and c) and have also been partly folded (Fig. 4b).

The seismic interpretations suggest the presence of two thrust sheets defined by the reflective Subbetic Jurassic packages, each of them underlain by less reflective zones interpreted as Triassic evaporites that host the detachments (Fig. 4e). Using seismic velocity of 5300 m/s, the upper detachment level is located at a depth of around 2.7 km depth (c. 1 s TWT) and the lower at c. 6.6 km depth (c. 2.5 s TWT). The lower detachment is just above an apparently less deformed, reflective package presumably consisting of Prebetic units (Fig. 4e). Indications of these units are identified down to at least 3.5s TWT (c. 9.3 km), giving the minimum depth to basement which must be deeper. The two thrust sheets have displacements in the order of tens of kilometers and the interpreted geometries in the seismic are consistent with the box-fold structure on the surface (Figs. 4e and f).

The NW boundary of the IFTB sector coincides with a change in the structural style. The detachment-fold dominated zone passes into a domain characterized by NW-verging thrusts rooting into the deeper detachment. The change in style corresponds to the changes in

the syn-orogenic lithostratigraphy of the units, in particular, with the first appearance of the Langhian-Serravallian formations that characterize the MFTB and the FFTB (Fig. 3a).

4.2. Middle fold-and-thrust belt (MFTB)

The MFTB includes the area of Sierra de Cabra (SC) and its surroundings (Figs. 3a and 6a). The SC consists mostly of Triassic to Palaeogene rocks of the Subbetic. The envelope of the MFTB surface topography is sharply interrupted in the northern limit of the Sierra, with a steep topographic drop from 1380 to 600 m (Fig. 3b). This slope break is associated with the mountain front, also considered as the MFTB/FFTB boundary (Figs. 3a and b). The overall structure of the SC is dominated by forethrusts up to 20 km long along their strike (Figs. 3a and 6a). The strikes of thrusts and reverse faults vary from N85ºE in the northernmost SC to N30ºE in the southernmost SC and the dip ranges from 45º to 90º in their present position (Figs. 3a, 5b, c, 6a, b, and c). Kilometric-scale, NNW-verging folds are developed in the thrust hanging walls (Figs. 5b and 6a). The slickenlines pitches are commonly > 45º, forming two clusters with roughly SE and SW plunging directions (Fig. 6b). Kinematic indicators (S-C structures and slickenfibers; Fig. 6b) show that the transport sense of the thrusts varies significantly, even for the same thrust. This kinematic variation could be assigned to the slip partitioning along curved thrust planes. Nevertheless, part of this variability may reflect some reactivation of these surfaces due to younger extensional events [Azañón et al., 2012].

Thrusts surfaces are interpreted to form an imbricate stack with a detachment located within the Triassic evaporites. Seismic data combined with well data imply the presence of a detachment between the Prebetic and Subbetic units, at c. 3.7 km depth (between 1 and 1.5 s TWT overall and at c. 1.4 s TWT, with depths constrained from the well H-1; Figs. 6f, g, and

7). In the underlying Prebetic unit is also deformed by thrusts that root into a basal detachment located on top of the Hercynian basement (Figs. 6f, g and 7). In the seismic strike-lines, lateral ramps are interpreted, particularly beneath the northern SC (Fig. 7a).

The OU is either completely eroded or not initially present within the SC, but outcrops around it to the W, E and N. Earlier Lower Miocene sediments show syn-growth features and are also affected by thrusting (Figs. 3a and 6a). Moreover, some Serravallian to Lower Tortonian sediments are also deformed by thrusts associated with the SC mountain front (Figs. 3a, 5b, c, 6a and f). Displacement along the thrusts within these younger units is small, but they do constrain the timing of the thrust system progression toward the NW (Figs. 6a and f).

4.2.1. Extensional structures

Apart from the contractional faults that define the main thrust system described above, two main extensional fault systems have been observed within the MFTB (Fig. 3a). They strike N-S to NW-SE (Fig. 6d) and WSW-ENE (Fig. 6e), respectively.

The approximately N-S to NW-SE striking, arc-perpendicular normal faults are seen both in the field and in the seismic images (Figs. 3a, 6a, d, 7a and c). These faults carry significant displacement and strongly control the current W and E limits of the SC with a topographic expression (> 400 m) and structural relief drop (Figs. 3a and c). The faults are planar to listric and they dip between 60º and 90º mostly outward from the SC (Fig. 6d). Slickenfibers show that they are dominantly dip-slip faults (Fig. 6d). Normal faults cut and displace the thrust surfaces, the Lower Miocene rocks and, in some cases, Quaternary sediments (Figs. 5d). The outcropping normal faults exhibit a maximum throw of c. 1.2 km, obtained by means of the Jurassic-Cretaceous boundary offset at cross-section. In addition to

the steep faults, low-angle normal faults of similar strike have been also reported [Azañón et al., 2012], although these have not been observed in our study area.

The minibasins formed by these N-S and NW-SE normal faults are filled with Langhian to Tortonian sediments, characterized by their poorly defined reflector character in the seismic images (e.g. the Cabra basin; Figs. 3a, c, 7a and c) The basin-fill sediments include the Lower Serravallian and OU deposits (Hernáiz et al., 1992). In the seismic images, the Lower Miocene sediments are interpreted to be cut by the normal faults and they have roughly wedge-shaped geometries indicative of growth strata (Fig. 7c). Consequently, the Langhian packages within the Cabra basin are interpreted as syn-extensional. Seismic images (Figs. 7b and 7c) suggest that the NW-SE striking normal faults have throws of up to ~1s TWT (c. 1.25 km) and are detached between the Subbetic and the Prebetic units at around 2.5 km (2s TWT). Throws of around 1.25 km are of a similar magnitude to the throw calculated from cross sections. A comparable listric fault system is interpreted ENE of the SC, although these faults do not penetrate below 0.4 km on seismic profiles (0.5 s TWT; Fig. 7a).

The other major normal fault system within the MFTB, defined by WSW-ENE, arc-parallel faults is likewise seen both at the surface and from seismic images. The Langhian timing of the onset of deformation along these faults is constrained by the interpreted growth structure of the OU packages in the seismic lines (Fig. 6g). The faults extend down to 2.65 km (c. 1 s TWT), accommodating significant NW-SE extension of the MFTB in c. NW-SE orientation (Figs. 6e, f and g). A maximum throw for the outcropping normal faults of c. 600 m is estimated by using the offset of the Jurassic-Cretaceous boundary on cross-sections. The throw from the seismic interpretation is c. 0.4s TWT, corresponding to c. 500m. Some of the SE-dipping normal faults, particularly in the S margin of the SC (Figs. 3a and 5e) may be inverted older thrust planes originated from the Lower Miocene deformation (Fig. 3a and 5e).

In addition to the main fault groups, Messinian to Recent, N-S striking, normal faults cut the WSW-ENE normal faults (Fig. 3a). These are not discussed further in this paper as they are not linked to the Langhian evolution of the FTB which is the focus of this study.

4.3. Frontal fold-and-thrust belt (FFTB)

With the exception of the transitional zones into the MFTB and the GB, the very poor quality of the seismic data from the FFTB has hindered the interpretation of the subsurface geology. Thus, the interpretation of the structural style in the FFTB is mainly derived from surface mapping. In contrast, the seismic images immediately to the N of the SC (MFTB/FFTB transition zone) show highly reflective packages, presumably made up of Prebetic or Subbetic limestones, as in the MFTB. The MFTB/FFTB transition zone coincides with both the northern limit of the exposed pre-orogenic sequences (Fig. 6g) and the southernmost OU outcrops. The dominant structures are inferred to be blind backthrusts accommodating significantly less shortening than in the MFTB (Figs. 3a, 6a, 6f and 6g). Despite the poor seismic quality, the presence of highly reflective Jurassic limestones permits estimation of minimum depths to basement in the transition zone (c. 6.2-6.9 km, i.e. c. 2.35-2.6s TWT).

North of this transitional zone, the FFTB is characterized by extensive outcrops of the OU and Upper Serravallian to Lower Tortonian sediments (Fig. 3a). The OU can be defined as a "block-in-matrix" unit [sensu Festa et al., 2010]: the blocks (olistholits) are composed of Jurassic limestones, and Triassic evaporites, wrapped in a plastic matrix of Langhian to Lower Serravallian deep water sediments (Fig. 5f) [Roldán et al., 1992; Roldán et al., 2012a]. The blocks have sub-angular to rounded shapes and show a gradual but clear size reduction toward the NNW: hectometric–scale blocks are common close to MFTB and their abundance

progressively decreases toward the GB (Fig. 3a). The OU is onlapped in the NW by shallow marine, Upper Serravallian to Lower Tortonian, calcareous sandstones (Fig. 3a). This package is further onlapped by Upper Tortonian to Messinian calcarenites and marls that thicken irregularly toward the N (Figs. 3a, 8a, b and c).

In the FFTB, the OU forms the cores to open, upright antiforms that on average strike N62ºE (Figs. 3a and 8d). These folds are doubly plunging, without a dominating vergence, and have kilometric-scale wavelengths, suggesting they are detachment folds (Figs. 3a, 8a and 8b). The OU presumably overlies the basement here because Lower Miocene or older rocks have not been identified at outcrop and are absent in wells in the GB farther to the NW (Figs. 3a and 8b). The Prebetic units that underlie the Subbetic thrust sheets and are encountered in well H-1 within the MFTB must, therefore, pinch out within the FFTB.

Another structural change occurs at the FFTB/GB boundary where mostly NW-verging imbricate structures are again interpreted in the seismic images, with some SE-verging backthrusts (see S83-48; Fig. 8b). These structures are blind thrusts detached at the bottom of the NW-thinning OU (Fig. 8b). Both folds and faults affect the Upper Serravallian to Lower Tortonian packages that we interpret to show syn-deformation growth structures with beds tilted up to 80º in the fold limbs (Figs. 3a, 8a and 8b).

4.4 Gualdalquivir Basin (GB)

The FFTB/GB boundary is marked by a topographic break that coincides with the boundary between the outcropping syn-orogenic Langhian-Lower Serravallian and the Upper Tortonian-Quaternary sediments (Fig. 8a). The seismic interpretation of the GB subsurface is constrained by surface geology and the well Río Guadalquivir N-1 (Figs. 8a, b and c). The GB form the fill to the foredeep depozone infill (see S83-40; Fig. 8b) [sensu DeCelles and

Giles, 1996]. In the Carmona-5 well (Fig. 2a), Upper Tortonian-Messinian sediments overlie the OU whilst in the well Río Guadalquivir N-1 the Tortonian to Messinian package overlies the Hercynian basement (Fig. 8c). The OU pinches out approximately along the line defined by Carmona-5 and Río Guadalquivir N-1 (Figs. 2a and 8c), which is in agreement with previous works [Martínez del Olmo and Martín, 2016].

Within the southwestern GB within the study area, the syn-orogenic packages are interpreted to be deformed and detached from the basement by NW-verging thrusts. The thrust displacements decrease NW-ward. Our interpretations show apparent differences in length between hanging wall and footwall ramps cutting Langhian-Lower Serravallian rocks (Fig. 8b). Out-of-plane thrust movements may explain this unusual interpreted pattern. We have not validated these interpretations by restoration because reliable markers are lacking, as seismic reflections do not necessarily correspond to formation boundaries, and because the data are not depth converted using reliable velocity data. The interpreted Upper Tortonian-Messinian package also shows thrusting, unconformities and growth structures such as onlaps onto the folds. Deformation intensity within the Upper Tortonian to Messinian sediments decreases toward the NW (Figs. 8b, 8f and 8e). Toward the NE part of the study area, the Hercynian basement is weakly deformed by reverse faults. Many of these structures possibly resulted from positive inversion of earlier normal faults inherited from the rifted paleomargin.

The current basement depth below the GB varies across and along the GB axis. The Tortonian-Messinian packages thicken irregularly toward the FFTB (Fig. 8b). The basement also deepens toward the SW, changing from 0.3 to 0.8 s TWT in the NE and from 0.5 to 1.2 s TWT further SW (Fig. 8b). Applying an average P-wave velocity of 2500 ms^{-1} (constrained from well Río Guadalquivir N-1), the GB infill is ca. 1.9 km thick in the deepest parts of the study area close to the boundary of the FFTB (Figs. 8b and 8c, see also Fig. 6 in Iribarren et al., [2009]).

4.5. Geometry of the external orogenic wedge

Combining previous works [e.g. Crespo-Blanc, 2007; 2008] with our data and interpretations, we suggest that the main detachment of the External Betic FTB is within the Triassic sequence under the IFTB and MFTB. However, we suggest that, as the Triassic evaporites pinch out, the detachment moves into the OU in the southern FFTB (Figs. 2a, 6f, 6g, 7a and 9a). In the MFTB, well and field data show that Subbetic and para-autochthonous Prebetic thrust sheets overlie Triassic evaporites (e.g. Figs. 6f, 7b and 8c) whereas the evaporites are absent in the wells in the GB and no indication of them are seen at outcrop NW of the MFTB/FFTB transition zone (Fig. 8b).Thus, the evaporites pinch-out along the Betics has been constrained using the well and outcrop data in our study and is consistent with previous works (Fig. 2a; e.g. Pérez-López and Pérez-Valera., 2007). The base of the thrust wedge base in the entire area is, despite the detachment being hosted by different units, likely to be along the basement top (Fig. 9a). The top-basement dip value (β) is only reliably constrained by the seismic and well data within the GB, giving a maximum depth of 2000 m and an average $\beta = 4^{o}$ (Fig. 9c). Under the MFTB and IFTB, we have been able to estimate β and the basement depths. Well Río Guadalquivir H-1 gives a reliable constraint to the absolute minimum depth to basement of >5000 m below the frontal MFTB. Furthermore, seismic interpretation suggests that depth to basement is 6-7 km (Figs. 6 and 7). The β value below the MFTB and IFTB is about 5^{o} (Fig. 9c). Given the large depth difference to top-basement between the GB and the MFTB, a significant increase of β must occur between GB and MFTB, forming a basement sloping step ("threshold") under the FFTB (Fig. 9c). The minimum β at this basement threshold must be ~ $12\text{-}13^{o}$ based on simple geometric relationships (Fig. 9c). Changing β value under the MFTB within reasonable limits will not affect our main conclusions or the requirement for a presence of a basement threshold below FFTB as the minimum depth to top-basement is constrained by well Río Guadalquivir H-1.

Based on regression analysis, the topographic relief envelope α is more than 0.2° over the GB and the FFTB, and more than 1° over the MFTB-IFTB, with the slope break located between the FFTB and MFTB (Fig. 9b). The present α, especially in the MFTB and IFTB, may have been different during the main wedge propagation and α = 1 is possibly a minimum value. However, we consider it to be a reasonable estimate of α at the time of the wedge propagation: the external orogenic wedge is still active evidenced by the presence of seismicity that can be associated with the advance of the Betic front (Sánchez-Gómez and Torcal-Medina, 2002). Hence, the tectonic wedge is likely to be reasonably close to equilibrium. Furthermore, and perhaps most importantly, changing the value within reasonable limits do not affect our main conclusions as discussed below.

The slope and base angle changes described above indicate that the wedge geometry varies significantly from MFTB-IFTB to GB. Several features described herein coincide spatially at the MFTB/FFTB transition: a) the lithological and deformational transition, b) the basement threshold, c) the slope break, and d) the pinch-out of the Triassic evaporites and the interpreted step-up of the main detachment from the evaporites to the OU.

5. Discussion

In this section, we will discuss the timing, the style, and the controlling factors of the external orogenic wedge evolution in the External Central Betics.

5.1 Aquitanian-Burdigalian deformation

Previous work concludes that the main thrusting within the External Zones of the Central Betics occurred during Lower Miocene (Aquitanian-Burdigalian; ca. 20 Ma) [Crespo-Blanc, 2007; 2008] and that the FTB front was subsequently dismantled generating the OU

during Langhian times (ca. 16-14 Ma) [Azañón et al., 2012; Roldán et al., 2012a, b; Rodríguez-Fernández et al., 2013] (Figs. 10a and b). However, post-Langhian extensional and contractional structures have been widely observed both in the Western Gibraltar Arc [Balanyá et al., 2012; Barcos et al., 2012; Jiménez-Bonilla et al., 2015a, b] and in the Eastern Betics [e.g. Giaconia et al., 2012; Pérez-Peña et al., 2010; Azañón et al., 2015]. Our observations from the IFTB-MFTB agree with these previous results. Because of the age of the OU, we suggest that orogenic contraction within the FFTB started after the Langhian (Fig. 10).

The main shortening in the study area may be equivalent to the main deformation events in other segments of the External Gibraltar Arc, which is responsible of the tectonic stacking of the Betic external zones [e.g. Expósito et al., 2012; Vitale et al., 2014]. Our results indicate that the main deformation in the Central Betics is slightly earlier than in the Western Betics (upper Aquitanian to lower Langhian, Fig. 10a) [e.g.; Crespo-Blanc and Frizon de Lamotte, 2006; Expósito et al., 2012]. This may be an expression of the W-migration of the Rif-Betic chains (Fig. 1).

5.2 Evidence for Langhian orogen-frontal collapse

The OU, a chaotic, mass wasting complex deposited c. 15-13 Ma in marine conditions, crops out mainly along the frontal MFTB and northwards. It is affected by the MTFB frontal thrusts and by folding farther into the FFTB. The significant extent of the OU in front of the MFTB, the concentration of hectometric-scale olistoliths close to the MFTB front, and the widespread Langhian normal faulting all imply that the mountain front was situated in the area of the present MFTB during the Upper Burdigalian-Lower Langhian and underwent rapid orogen-frontal gravitational dismantling (Fig. 10b). The MFTB/FFTB

boundary and the topographic slope break overlie the basement threshold (Figs. 9a, b and c). The basement threshold may be located at an ancient major fault scarp to a normal fault inherited from the Mesozoic rifting of the Subbetic paleomargin. The presence of a basement threshold, combined with the thinning out of evaporites suggests that wedge basal properties varied across the orogenic strike. These variations in turn led directly to the topographic build-up in the MFTB, triggering the Langhian gravitational collapse and consequent formation of the OU.

5.2.1. Application of the critical taper model on the Langhian gravitational collapse

According to the review of Graveleau et al., [2012], the critical taper theory and modelling results show that multiple causes can be involved in the transition from "regular" wedge propagation to build-up and subsequent gravitational collapse. At a wedge scale, some of the most important causes include vertical, lateral and transport-parallel changes in material strength of the thrust wedge (lithological/facies changes), changes in the detachment frictional properties, and the inherited sub-detachment topography and structure [e.g. Davis et al., 1983; Dahlen, 1984; 1990; Calassou et al., 1993; Macedo and Marshak, 1999; Cotton and Kovi, 2000; Suppe, 2007; Bahroudi and Koyi, 2003; Luján et al, 2003; Miyakawa et al., 2010; Graveleau et al., 2012]. Mass wasting recorded by olistostrome formation may itself directly affect the subsequent orogenic wedge development by changing the overall wedge geometry [Smit et al., 2010]. We focus on the potential effects and interactions of the observed basal friction and β variations on the Langhian evolution of the Central Betics FTB below (Figs. 11a and b).

We approximate that the IFTB/MFTB deformed initially very close to critical taper and that the present α value is reasonably close to the α during Aquitanian-Langhian (Fig. 11c). The change in the structural style from detachment folds to forward vergent thrusts conforms to critical taper models where the basal friction angle Φ_b increases [e.g. Dahlen,

1984; Argawal and Argawal, 2002]. Detachment folds above weak evaporitic/shaly detachments are also well known from natural cases such as the Jura Mountains [Burkhard and Sommaruga, 1998; Smit et al., 2003]; the Appalachians [Mount, 2014]; the outer Niger Delta toe thrust belt [Cobbold et al., 2009]; and Northern Israel [Gradmann et al., 2005]. The effect of β is more controversial. Critical taper theory [e.g. Dahlen, 1984] predicts that, all other parameters being equal, moderately increasing β will not increase α in non-cohesive wedges unless the wedge stability field is already very narrow. However, some modelling results imply that β might increase α [e.g.; Koyi and Vendeville, 2003].

Using equations 9, 17 and 19 of Dahlen [1984], we illustrate the possible effects of Φ_b and β changes at the FFTB basement threshold on the wedge stability and behaviour (Figs. 11b and c). Pore fluid factors of λ=0.6 and λ_b=0.75 are used; other realistic lower pore fluid factors (e.g. λ=0.6 and λ_b=0.85) yield approximately similar results as long as $\lambda_b > \lambda$. The effect of cohesion is estimated to be negligible. The Fig. 11c illustrates two possible end-member scenarios for the ~Langhian evolution of the FTB front, both of which have a basement threshold (β increase from ~5° to 12°) but the role of the pinch-out of the Triassic evaporites vary.

In scenario 1 (path I-III in Fig. 11c), Φ_b increases due to the pinch-out of the Triassic before the wedge reaches the basement threshold. In this end-member case,,an increase in Φ_b causes shrinkage of the wedge stability field and raises the taper angle by increasing α to ~3° (path I). α may increase even more if Φ_b approaches unity with Φ (no weak substrate). As the frontal part of the wedge progresses onto the basement threshold (β=12°), it enters the overcritical (extensional) domain (path II) as illustrated in Fig. 11c. As a result, the orogenic front collapses (path III) creating the OU and the orogen-parallel normal faults form as α evolves towards critical taper.

In scenario 2 (path IV), β increases without considerable changes in basal frictional properties. In this case, the frontal FTB encounters the basement threshold without Triassic pinch-out, i.e. no change in Φ_b (path IV); this scenario is the other end-member for this particular system. However, we consider it to be unlikely as a pinch-out is interpreted from seismic and well data (Figs. 6f, g, 7a and b). This end-member scenario will not itself increase α and cause collapse because the stability field remains unchanged. Subsequent or simultaneous shrinking in the stability field for the orogenic wedge due to an increase in Φ_b would be needed to bring the frontal FTB into the extensional domain.

Scenario 1) is more likely than scenario 2) because we interpret that the Triassic evaporites thickness diminishes significantly from the IFTB to the MFTB (Figs. 6f, g, 7a and b), although in reality the tempo-spatial relationships between the basal friction and β are probably somewhere between 1) and 2). Nevertheless, an orogen-frontal collapse following significant topographic build-up, caused by a combination of increase in both Φ_b and β, is the most likely explanation for the widespread extent of the OU, the large olistolith size, and the extensive orogen-parallel normal faulting observed throughout the frontal part of the Langhian FTB.

Slab dynamics/rollback and/or mantle delamination in the Betics and Rif chain development need to be briefly discussed in this context as these processes have played a crucial role in the post-Langhian development of the Betic FTB. Late Miocene to Holocene slab rupture and associated delamination resulted in topographic uplift and typical volcanism [Lonergan and White, 1997; Duggen et al., 2003; Booth-Rea et al., 2007; García-Castellanos and Villaseñor, 2011; Bezada et al., 2013; Thurner et al., 2014; Mancilla et al., 2015]. This mechanism also drove Late Miocene and younger extension and volcanism in the external thrust belt in the eastern Betics [Pérez-Valera et al., 2013] and crustal-scale boudins [Mancilla et al., 2015]. However, as the slab effects were more pronounced east of our study

area and younger than the proposed wedge stagnation, we consider slab dynamics to have little impact to our results illustrating the importance and interaction of the local basement properties: a local dip increase has a potential to significantly add to the effects of increasing Φ_b, and to the magnitude of the subsequent collapse of the orogenic front.

As a summary, we suggest that i) the front of the orogenic wedge had migrated to the MFTB area by the Langhian, and ii) the main shortening and wedge propagation (early Miocene) and the post-Langhian shortening and propagation migrating further NW were in the study area separated by a intra-Langhian "stagnation" phase where the wedge propagation was temporarily disturbed by local topographic build-up and subsequent collapse. This stagnation and the building up to a supra-critical state of the wedge taper at the wedge front was caused by a combination of the basal dip steepening and pinch-out of the Triassic evaporites. The topographic build-up and the resulting collapse coincided in time and space with the formation of the OU and the minibasins, likely caused by the Langhian stagnation.

5.3 Post-Langhian evolution

Post-Langhian deformation is identified throughout the area, and although it is not the focus of this paper, this phase is briefly described below. The Langhian-Tortonian sediments within the MFTB, FFTB and GB, including the OU which resulted from the frontal collapse, are affected by thrust deformation and folding [see also Roldán et al., 2012a, b]. Therefore, shortening deformation lasted until at least the Messinian as the orogenic front and its foreland basin propagated farther towards NW. In addition, the positive inversion of pre-existing basement normal faults in the GB (Fig. 8b) could be associated with seismically active faults reported in this area (magnitudes 1-6 [e.g. Sánchez-Gómez and Torcal-Medina, 2002; Pedrera et al., 2013; Sánchez-Gómez et al., 2014]). It is noteworthy that the

earthquakes distributed along the FFTB-GB boundary show focal mechanisms congruent with the ENE-WSW reverse faults and NNW-SSE normal faults [Sánchez-Gómez and Torcal-Medina, 2002]. It appears that the strain partitioning into NE-SW stretching and NNW-SSE shortening may still be currently active in the frontal FTB of the Central Betics. Moreover, post-Langhian NNW-SSE stretching seems to have taken place.

The new detachment under the FFTB developed within the OU, which is mostly composed of limestone clasts in a matrix of marls, gypsum and clays (Fig. 11a). The rheological change between the Triassic evaporites and the OU, the latter presumably having higher internal friction than the evaporites, may have contributed to the change on the structural style between the MFTB and the FFTB, but the detailed investigation of this is outside the scope of this paper. The OU thickness is interpreted to change from 200 m in the MFTB to around 1.5 km in the FFTB where it was deposited in the Langhian foreland basin. As a result, the double verging detachment folds in the FFTB would be controlled by the detachment within the OU. The OU pinches out within or possibly before the GB, associated with the dying out of NW-verging fault-propagation folds. These folds, however, together with some basement inversion only accommodate a limited amount of shortening, effectively marking the end of the main wedge propagation in this area. Inversion of basement faults is interpreted to accommodate some of the shortening, whereas there is no evidence of basement involvement in the Western Betics, where a thick weak substrate is still present farther NW with respect to the FTB deformation front [González-Castillo et al., 2015] (Fig. 2a).

The progressive younging of the depocenters NNW-ward is consistent with a post-Langhian NNW-ward progression of the FTB, probably coeval with tightening of previous shortening structures in the MFTB and IFTB (Fig. 10b; see also Crespo-Blanc [2007; 2008]).

Although a further subsidence analysis must be considered, it appears that the GB subsidence may have continued until the Upper Miocene, migrating progressively toward the NW.

6. Conclusion

The main conclusions of this study can be summarised as:

- Four structural domains have been distinguished across the Central Betics from the inner FTB to the Guadalquivir foreland basin. They differ in their prevailing type and vergence of structures, age of deformation and nature of the involved rock formations.

- The observed structural style changes and the Langhian orogen-frontal collapse are explained through the critical taper theory and result largely from changes in the wedge basal properties; the FTB progression slowed down in the area of the present MFTB during the Upper Burdigalian-Lower Langhian, with a rapid increase in topography and subsequent orogen-frontal collapse, induced by changes in the basal friction and dip angles. Simultaneously, N-S normal faults accommodated arc-parallel stretching, some of which have remained are active into the Quaternary;

- The frontal collapse was a major contributor to the formation of the Olistostromic Unit. The OU went to become the weak substrate to subsequent thrusts and enabled the renewed NW progression of the FTB after the Langhian, once the critical taper was re-established; and

- The FTB front migrated further into the present Guadalquivir Basin, with the foreland depocenter also migrating NW-wards.

Acknowledgements

This research is supported by projects RNM-0451 and CGL2013-46368. We are grateful to Guillermo Booth Rea, Andrea Artoni and an anonymous reviewer for their very helpful comments. Tectonics editors, Claudio Faccenna and Whitney Behr, are also thanked for their assistance. Rob Butler is thanked for checking the English of the manuscript. Seismic images were downloaded from www.ign.es and http://info.igme.es/infogeof/ and the Spanish Ministry of Energy and Industry is gratefully acknowledged for making the images publically available.

REFERENCES

Argawal, K.K. and Argawal, G.K., (2002), Analogue sandbox models of thrust wedges with variable basal frictions. Gondwana Research, 5, 641-647. doi: 10.1016/S1342-937X(05)70635-3

Azañón, J.M., Roldán, F.J. and Rodríguez-Fernández, J., (2012), Fallas y despegues extensionales en el Subbético Central: implicaciones en la evolución Neógena de Las Zona Externa de la Cordillera Bética. Geogaceta, 52, 13-16.

Azañón, J.M., Galve, J.P., Pérez-Peña, J.V., Giaconia, F., Carvajal, R., Booth-Rea, G., Jabaloy, A., Vázquez, M., Azor, A. and Roldán, F.J., (2015), Relief and drainage evolution during the exhumation of the Sierra Nevada (SE Spain): Is denudation keeping pace with uplift? Tectonophysics 663, 19-32. doi: 10.1016/j.tecto.2015.06.015.

Bahroudi, A. and Koyi, H., (2003), The effect of spatial distribution of Hormuz salt on deformation style in the Zagros fold and thrust belt: an analogue modelling approach. Journal of the Geological Society of London, 160, 719-733. doi: 10.1144/0016-764902-135

Bahroudi, A., Koyi, H.A. and Talbot, C.J., (2003), Effect of ductile and frictional décollements on style of extension. Journal of Structural Geology 25 (9), 1401-1423. doi: 10.1016/S0191-8141(02)00201-8.

Balanyá, J. C. and García-Dueñas, V., (1987), Les directions structurales dans le Domaine d'Alborán de part et d'autre du Détroit de Gibraltar. C. R. .Acad. Sc., París, 304,304: 929-933.

Balanyá, J. C., Crespo-Blanc, A., Díaz-Azpiroz, M., Expósito, I. and Luján, M., (2007), Structural trend line pattern and strain partitioning around the Gibraltar Arc accretionary wedge: Insights as to the mode of orogenic arc building. Tectonics 26, 1-19. doi.org/10.1029/2005TC001932.

Balanyá, J. C., Crespo-Blanc, A., Díaz-Azpiroz, M., Expósito, I., Torcal, F., Pérez-Peña, J. V. and Booth-Rea, G., (2012), Arc-Parallel vs back-arc extension in the Western Gibraltar arc: Is the Gibraltar forearc still active? Geologica Acta 10, 249-263. doi:10.134/105.000001771.

Barcos, L., Expósito,I., Balanyá, J.C. and Díaz-Azpiroz, M., (2012), Levantamiento tectónico asociado a transpresión en el Penibético de la Sierra del Valle de Abdalajís (Béticas): análisis estructural y geomorfológico. Geo-Temas 13, 507–601.

Bezada, M.J., Hymphreys, E.D., Toomey, D.R., Harnafi, M., Dávila, J.M. and Gallart, J., (2013), Evidence for slab rollback in westernmost Mediterranean from improved upper mantle imaging. Earth Planet Sc Lett 368, 51-60.

Booth-Rea, G., Ranero, C.R., Grevemeyer, I. and Martínez-Martínez, J.M., (2007), Crustal types and tertiary tectonic evolution of the Alborán sea, western Mediterranean. Geochemistry, Geophysics, Geosystems 8, (10), Q10005. doi: 10.1029/2007GC001639

Booth-Rea, G., Martínez-Martínez, J.M. and Giaconia, F., (2015), Continental subduction, intracrustal shortening, and coeval upper-crustal extension P-T evolution of subducted south Iberian paleomargin metapelites (Betics, SE Spain). Tectonophysics 663, 122-139. doi: 10.1016/j.tecto.2015.08.036

Buchanan, P. G., and McClay, K. R., (1991), Sandbox experiments of inverted listric and planar faults systems. In: P.R. Cobbold (ed.) Experimental and Numerical Modeling of Continental Deformation. Tectonophysics 188, 97-115.

Buforn, E., de Galdeano, C.S. and Udías, A., (1995), Seismotectonics of the Ibero-Maghrebian region. Tectonophysics 248, 247-261. doi: 10.1016/0040-1951(94)00276-F

Burkhard, M., and Sommaruga, A., (1998), Evolution of the western Swiss Molasse basin: structural relations with the Alps and the Jura belt. Geological Society, London, Special Publications, 134, 279-298. doi:10.1144/GSL.SP.1998.134.01.13.

Calassou, S., Larroque, C and Malavieille, J., (1993), Transfer zones of deformation in thrust wedges; an experimental study. Tectonophysics, 221, 325-344. doi: 10.1016/0040-1951(93)90165-G

Chourak, M., Corchete, V., Badal, J., Gómez, F. and Serón, F.J. (2005), Shallow seismic velocity structure of the Betic Cordillera (Southern Spain) from modelling of rayleigh wave dispersion. Surveys in Geophysics 26, 481-504. doi: 10.1007/s10712-005-7260-4

Cobbold, P.R., Clarke, B.J. and Loseth, H., (2009), Structural consequences of fluid overpressure and seepage forces in the outer thrust belt of the Niger Delta. Petroleum Geoscience 15, 2-15. doi: 10.1144/1354-079209-784

Comas, M.C., Platt, J.P., Soto, J.I. and Watts, A.B., (1999), The origin and tectonic history of the Alborán basin: insights from Leg 161 results, in: R. Zahn, M.C. Comas, A. Klaus (Eds.), Proceeding of the Ocean Drilling Program, Scientific Results, 161, pp. 555-579.

Codegone, G., Festa, A., Dilek, Y. and Pini, G. A., (2012), Small-scale polygenic mélanges in the Ligurian accretionary complex, Northern Apennines, Italy, and the role of shale diapirism in superposed mélange evolution in orogenic belts. Tectonophysics 568-569, 170-184. doi : 10.1016/j.tecto.2012.02.003

Cotton, J. and Koyi, H., (2000), Modeling of thrust fronts above ductile and frictional detachments: application to structures in the Salt Range and Potwar Plateau, Pakistan. Geological Society of America Bulletin, 112, 351-363. doi: 10.1130/0016-7606(2000)112<0351:MOTFAD>2.3.CO;2

Crespo-Blanc, A., (2007), Superimposed folding and oblique structures in the palaomargin-derived units of the Central Betics (SW Spain). Journal of the Geological Society of London, 164, 621-636. doi: 10.1144/0016-76492006-084

Crespo-Blanc, A., Balanyá, J.C., Expósito, I., Luján, M. and Díaz-Azpiroz, M., (2007), Acreción Miocena del Dominio Sudibérico y del Complejo de los Flyschs (Arco de Gibraltar): Una revisión a partir de las propuestas de V. García-Dueñas. Revista de la Sociedad Geológica de España 20 (3-4), 135-152.

Crespo-Blanc, A., (2008), Recess drawn by the internal zone outer boundary and oblique structures in the paleomargin-derived units (Subbetic Domain, central Betics): An analogue modelling approach. Journal of Structural Geology 30, 65-80. doi: 10.1016/j.jsg.2007.09.009

Crespo-Blanc, A. and Campos, J., (2001), Structure and kinematics of the South Iberian paleomargin and its relationship with the Flysch Trough units: extensional tectonics within the Gibraltar arc fold-and-thrust belt (western Betics). Journal of Structural Geology 23, 1615–1630. doi: 10.1016/S0191-8141(01)00012-8

Crespo-Blanc, A. and Frizon de Lamotte, (2006), Structural evolution of the external zones derived from the Flysch Trough and the South Iberian and Maghrebian paeomargins around the Gibraltar arc: A comparative study. Bull. Soc. Geol. France, 177, 5, 267-282.

Dahlen, F.A., (1984), Noncohesive critical Coulomb wedges: an exact solution. Journal of Geophysical Research, 89, 10125-10133. doi: 10.1029/JB089iB12p10125

Dahlen, F.A., (1990), Critical taper model of fold-and-thrust belts and accretionary wedges. Annual Review of Earth and Planetary Sciences, 18, 55-99. doi: 10.1146/annurev.ea.18.050190.000415

Davis D.M. and Engelder T. (1985), The role of salt in fold-and-thrust belts. Tectonphysics, 119, 67-88.

Davis, D., Suppe, J. and Dahlen, F. A., (1983), Mechanics of fold-and-thrust belts and accretionary wedges. Journal of Geophysical research, 88, 1153-1172. doi: 10.1029/JB088iB02p01153.

DeCelles, P. G. and Giles K. A., (1996), Foreland basin systems. Basin Research 8, 105-123. doi: 10.1046/j.1365-2117.1996.01491.x

DeCelles, P. G., (2012), Foreland Basin Systems Revisited: Variations in Response to Tectonic Settings, Tectonics of Sedimentary Basins. John Wiley & Sons, Ltd., pp. 405–426. doi: 10.1002/9781444347166.ch20

Díaz de Neira, J. A., Enrile, A., Hernáiz, P. P. and López-Olmedo, F., (1992), Geological map. Sheet Alcalá la Real, 990. Instituto Tecnológico Geominero de España, scale 1:50,000.

Duggen, S., Hoernle, K., van den Bogaard, P., Rupke, L. and Morgan, J.P., (2003), Deep roots of the Messinian salinity crisis. Nature 422, 602-606.

Durand-Delga, M., Rossi, P., Olivier, P. and Puglisi, D., (2000), Situation structurale et nature ophiolitique de roches basiques jurassiques associées aux flyschs maghrébins du Rif (Maroc) et de Sicile (Italie). Comptes-Rendus de l'Académie des Sciences de Paris, 331, 29-38.

Expósito, I., Balanyá, J.C., Crespo-Blanc, A., Díaz-Azpiroz, M. and Luján M., (2012), Overthrust shear folding and contrasting deformation styles in a multiple decollement setting, Gibraltar Arc external wedge. Tectonophysics 576-577, 86-98. doi: 10.1016/j.tecto.2012.04.018

Fagereng, Å., (2011), Wedge geometry, mechanical strength, and interseismic coupling of the Hikurangi subduction thrust, New Zealand. Tectonophysics, 507, 26-30. doi: 10.1016/j.tecto.2011.05.004

Festa, A., Pini, G.A., Yildirim, D. and Giulia, C., (2010), Mélanges and mélange-forming processes: a historical overview and new concepts. International Geology Review, 52(10), 1040-1105. doi: 10.1080/00206810903557704

Gallastegui, J., Pulgar, J. A. and Álvarez-Marrón, J., (1997), 2-D seismic modelling of the Variscan foreland thrust and Fold belt crust in NW Spain from ESCIN-1 deep seismic reflection data. Tectonophysics, 269, 21-32. doi: 10.1016/S0040-1951(96)00166-7.

García-Castellanos, D., and Villasenor, A., 2011. Messinian salinity crisis regulated by competing tectonics and erosion at the Gibraltar arc. Nature 480, 359-U108.

García-Cortés, A., (1992), Geological map. Sheet Alcaudete, 968. Instituto Tecnológico Geominero de España, scale 1:50,000.

García-Dueñas, V., Balanyá, J.C. and Martínez-Martínez, J.M. (1992), Miocene extensional detachments in the outcropping basement of the northern Alboran Basin (Betics) and their tectonic implications. Geo Mar. Lett., 12, 88-95.

García-Hernández, M., López-Garrido, A. C., Rivas, P., Sanz de Galdeano, C. and Vera, J. A., (1980), Mesozoic paleogeographic evolution the External Zones of the Betic Cordillera. Geologie en Mijnbow 59, 155-168.

Giaconia, F., Booth-Rea, G., Martínez-Martínez, J.M., Azañón, J.M., Pérez-Peña, V., Pérez-Romero, J. and Villegas, I., (2012), Geomorphic evidence of active tectonics in the Sierra Alhamilla (eastern Betics, SE Spain). Geomorphology 145–146, 90-106. http://dx.doi.org/10.1016/j.geomorph.2011.12.043

González-Castillo, L., Galindo-Zaldívar, J., Pedrera, A., Martínez-Moreno, F.J. and Ruano P., (2015), Shallow frontal deformation related to active continental subduction: structure and recent stresses in the westernmost Betic Cordillera. Terra Nova 27, 114-121. doi: 10.1111/ter.12138

Gradmann, S., Hübscher, C., Ben-Avraham, Z., Gajewski, D. and Netzeband, G., (2005), Salt tectonics off northern Israel. Marine and Petroleum Geology 22, 597-611. doi: 10.1016/j.marpetgeo.2005.02.001

Graveleau, F., Malavieille, J. and Dominguez, S., (2012), Experimental modelling of orogenic wedges: a review. Tectonophysics, 538-540, 1-66.

Hernáiz, P. P., Díaz de Neira, J. A., Enrile, A. and López-Olmedo, F., (1992), Geological map. Sheet Lucena, 989. Instituto Tecnológico Geominero de España, scale 1:50,000.

Iribarren, L., Vergés, J. and Fernández, M., (2009), Sediment supply from the Betic-Riforogen to basins through Neogene. Tectonophysics 475 (1), 68-84. doi: 10.1016/j.tecto.2008.11.029

Jiménez-Bonilla, A., Balanyá, J.C., Expósito, I. and Díaz-Azpiroz, M., (2011), Superposición de estructuras y controles tectónicos en el desarrollo del límite SW de la depresión de Ronda (Subbético y Complejo de los Flyschs, Béticas). Geogaceta, 50, 23-26.

Jiménez-Bonilla, A., Balanyá, J.C., Díaz-Azpiroz, M. and Expósito, I., (2012), Control tectónico de las diferencias de relieve estructural y topográfico en el margen NE de la Depresión de Ronda (Béticas Occidentales). Geo-Temas. 13, 499-503.

Jiménez-Bonilla, A., Expósito, I., Balanyá, J.C., Díaz-Azpiroz, M. and Barcos, L., (2015a), The role of strain partitioning on intermontane basin inception and isolation, External Western Gibraltar Arc. Journal of Geodynamics 92, 1-17.

Jiménez-Bonilla, A., Expósito, I., Balanyá, J.C., Barcos, L. and Díaz-Azpiroz, M., (2015b), Structure and kinematics of Subbetic and related mélange-like units NW of Ronda Basin (Western Betics): Evidences for a transpressional structural high in the frontal thrust-and-fold belt. Geogaceta 57, 27-30.

Jiménez-Bonilla, A., Balanyá, J.C., Expósito, I., Crespo-Blanc, A., Torvela, T., Díaz-Azpiroz, M. and Barcos, L., (2016), Miocene strain partitioning within the fold-and-thrust belt of the Central Betics (Gibraltar Arc orogenic system). Geogaceta 59, 23-26. ISSN (Internet): 2173-6545.

Koyi, H.A. and Vendeville, B.C., (2003), The effect of décollement dip on geometry and kinematics of model accretionary wedges. Journal of Structural Geology, 25, 1445-1450. doi: 10.1016/S0191-8141(02)00202-X

Krzywiec P., and Verges J. (2007), Role of the foredeep evaporites in wedge tectonics and formation of triangle zones: comparison of the Carpathian and Pyrenean thrust fronts. In Lacombe, O., Lavé, J., Roure, F.M., Verges, J. (Eds.), Thrust Belts and Foreland Basins, From Fold Kinematics to Hydrocarbon Systems. Frontiers in Earth Sciences, Springer 385-396.

Leyva, F., (1975), Geological map. Sheet Espejo, 944. Instituto Tecnológico Geominero de España, Madrid, scale 1:50,000.

Liu, H., McClay, K.R. and Powell, D., (1992), Physical models of thrust wedges. In: McClay, K.R., (Ed.), Thrust Tectonics. Chapman and Hall, London, pp. 71-81.

Lonergan. L., and White, N., (1997), Origin of the Betic-Rif mountain belt. Tectonics 16, 504-522. doi: 10.1029/96TC03937

Lucente, C.C., and Pini, G.A., (2008), Basin-wide mass-wasting complexes as markers of the Oligo-Miocene foredeepaccretionary wedge evolution in the Northern Apennines, Italy. Basin Research 20, 49-71. doi: 10.1111/j.1365-2117.2007.00344.x

Luján, M., Storti, F., Balanyá, J.-C., Crespo-Blanc, A. and Rossetti, F., (2003). Role of decollement material with different rheological properties in the structure of the Aljibe thrust imbricate (Flysch Trough, Gibraltar Arc): an analogue modelling approach. Journal of Structural Geology, 25, 867-881. doi: 10.1016/S0191-8141(02)00087-1

Luján, M., Crespo-Blanc, A. and Balanyá, J.C., (2006), The Flysch Trough thrust imbricate (Betic Cordillera): a key element of the Gibraltar Arc orogenic wedge. Tectonics 25, TC6001. doi: 10.1029/2005TC001910.

Macedo, J.. and Marshak, S., (1999), Controls on the geometry of fold thrust belt salients. Geological Society of America Bulletin 111, 1808-1822. doi:10.1130/0016 - 7606(1999)1112.3.CO;2

Maldonado, A., Somoza, L. and Pallarés, L., (1997), The Betic orogen and the Iberian-African boundary in the Gulf of Cadiz: geological evolution (central North Atlantic). Marine Geology 155, 9-43. PII: S0025-3227(98()00139-X

Mancilla, F.D., Booth-Rea, G., Stich, D., Perez-Pena, J.V., Morales, J., Azañon, J.M., Martin, R. and Giaconia, F., (2015), Slab rupture and delamination under the Betics and Rif constrained from receiver functions. Tectonophysics 663, 225-237.

Martínez del Olmo, W and Martín, D., (2016), El Neógeno de la cuenca Guadalquivir-Cádiz (Sur de España). Revista de la Sociedad Geológica de España 29 (1), 35-58.

Medialdea, T., Vegas, R., Somoza, L., Vázquez, J. T., Maldonado, A., Díaz-del-Río, V., Maestro, A., Córdoba, D. and Fernández-Puga, M. C., (2004), Structure and evolution of the "Olistostrome" complex of the Gibraltar Arc in the Gulf of Cádiz (eastern Central Atlantic): evidence from two long seismic cross-sections. Marine Geology, 209, 173-198. doi: 10.1016/j.margeo.2004.05.029

Medialdea, T., Somoza, L., Pinheiro, L. M., Fernández-Puga, M. C., Vázquez, J. T., León, R. and Ivanov, M. K., (2009), Tectonics and mud volcano development in the Gulf of Cádiz. Marine Geology 261, 48-63. doi: 10.1016/j.margeo.2008.10.007

Michard, A., Saddiqi, O., Chalouan, A. and Frizon de Lamotte, D., (2008), Continental Evolution: The Geology of Morocco. Structure, Stratigraphy, and Tectonics of the Africa-Atlantic- Mediterranean Triple Junction. Springer-Verlag, Berlin Heidelberg 116-404 pp.

Mitchum, R.M.,J. and P.R. Vail, (1977), Seismic stratigraphy and global changes of sea level; Part 7, Seismic stratigraphic interpretation procedure: AAPG Memoir 26, p. 135-143.

Miyakawa, A., Yamada, Y. and Matsuoka, T., (2010), Effect of increased shear stress along a plate boundary fault on the formation of an out-of-sequence thrust and a break in surface slope within an accretionary wedge, based on numerical simulations. Tectonophysics, 484, 127-138. doi: 10.1016/j.tecto.2009.08.037

Mount, V. S., (2014), Structural style of the Appalachian Plateau fold belt, north-central Pennsylvania. Journal of Structural Geology, 69, 284-303. doi: 10.1016/j.jsg.2014.04.005

Pedrera, A., Ruíz-Constán, A., Marín-Lechado, C., Galindo-Zaldívar, J., González, A. and Peláez, J.A., (2013), Seismic transpressive basement faults and monocline development in a foreland basin (Eastern Guadalquivir, SE Spain). Tectonics 63, 1571-1586. doi: 10.1002/2013TC003397

Pérez-Valera, F. and Pérez-López, A., (2003), Estratigrafía y tectónica del Triásico sudibérico al sureste de Calasparra (Murcia). Revista de la Sociedad Geológica de España 1-2, 35-50.

Perez-Valera, L.A., Rosenbaum, G., Sanchez-Gomez, M., Azor, A., Fernandez-Soler, J.M., Perez-Valera, F. and Vasconcelos, P.M., (2013). Age distribution of lamproites along the Socovos Fault (southern Spain) and lithospheric scale tearing. Lithos 180.

Pérez-López, A. and Pérez-Valera, (2007), Palaeogeography, facies and nomenclature of the Triassic units in the different domains of the Betic Cordillera (S Spain). Palaeogeography, Palaeoclimatology, Palaeoecology 254, 3, 606-626. doi:10.1016/j.palaeo.2007.07.012.

Pérez-Peña, J.V., Azor, A., Azañón, J.M. and Keller, E.A., (2010), Active tectonics in the Sierra Nevada (Betic Cordillera, SE Spain): insights from geomorphic indexes and drainage pattern analysis. Geomorphology 119, 74-87. doi: 10.1016/j.geomorph.2010.02.020

Platt, J. P., Behr, W. M., Johanesen, K. and Williams, J. R., (2013), The Betic-Rif Arc and its orogenic hinterland: a review. Annual Review of Earth and Planetary Sciences 41, 313-357. doi: 10.1146/annurev-earth-050212-123951

Poblet, J., and Lisle, R. J., (2011), Kinematic Evolution and Structural Styles of Fold-and-Thrust Belts. Geological Society, London, Special Publications, 349, 1-24. doi: 10.1144/SP349.1.

Rodríguez-Fernández, J., Roldán, F. J., Azañón, J. M. and García-Cortés, A., (2013), El colapso gravitacional del frente orogénico alpino en el Dominio Subbético durante el Mioceno medio-superior: El Complejo Extensional Subbético. Boletín Geológico y Minero 124 (3): 477-504.

Roldán, F.J. and García-Cortés, A., (1988a), Implicaciones de materiales triásicos en la Depresión del Guadalquivir, Cordilleras Béticas (Prov. de Córdoba y Jaén). II Congreso Geológico de España. Granada 1, 189-192

Roldán, F. J. and Divar, J., (1988b), Geological map. Sheet Castro del Río, 966. Instituto Tecnológico Geominero de España, scale 1:50,000.

Roldán, F. J., Ruíz-Ortiz, P. A. and Molino, J. M., (1988c), Geological map. Sheet Baena, 967. Instituto Tecnológico Geominero de España, scale 1:50,000.

Roldán, F. J., Lupiani, E. and Villalobos, M., (1992), Geological map. Sheet Castro del Río, 945. Instituto Tecnológico Geominero de España, scale 1:50,000.

Roldán, F.J., Rodríguez-Fernández, J. and Azañón, J.M. (2012a), La Unidad Olistostrómica, una formación clave para entender la historia neógena de las Zonas Externas de la Cordillera Bética, Geogaceta, 52, 9-12.

Roldán, F. J., Rodríguez-Fernández, J., Villalobos, M., Lastra, J., Díaz-Pinto, G. and Pérez-Rodríguez, A. B. (2012b), Zonas: Subbético, Cuenca del Guadalquivir y Campo de Gibraltar. In: GEODE. Mapa Geológico Digital Continuo de España. Sistema de Información Geológica Continua: SIGECO. IGME. Navas, J. (ed.). Available in: http://cuarzo.igme.es/sigeco.default.htm.

Sánchez-Gómez, M. and Torcal-Medina, F. (2002), Primer centenario del Observatorio de Cartuja. Cien Años de Sismologia en Granada, 8-11.

Sánchez-Gómez, M., Peláez, J.A., García-Tortosa, F.J., Pérez-Valera, F. and Sanz de Galdeano C., (2014), La serie de Torreperogil (Jaén, Cuenca del Guadalquivir Oriental): Evidencias de deformación tectónica en el área epicentral. Revista de la Sociedad Geológica de España 27 (1), 301-318.

Serrano, I., Torcal, F. and Martín, J.B., (2015), High resolution seismic imaging of an active fault in the eastern Gaudalquivir Basin (Betic Cordillera, Southern Spain). Tectonophysics 660, 79-91. doi: 10.1016/j.tecto.2015.08.020

Sierro, F. J., González-Delgado, J. A., Dabrio, C. J., Flores, J. A. and Civis, J., (1996), Late Neogene depositional sequences in the foreland basin of Guadalquivir (SW Spain). In: Friend, P., and Dabrio, C. J., (eds) Tertiary Basins of Spain: The stratigraphic record of crustal kinematics. Cambridge University Press. 339-345.

Simpson, G. D. H., (2009), Mechanical modelling of folding versus faulting in brittle-ductile wedges. Journal of Structural Geology 31, 369-381. doi: 10.1016/j.jsg.2009.01.011

Smit, J.H.W., Brun, J.P. and Sokoutis, D., (2003), Deformation of brittle-ductile thrust wedges in experiments and nature. Journal of Geophysical Research 108, doi:10.1029/2002JB002190

Smit, J., Burg, J.-P., Dolati, A. and Sokoutis, D., (2010), Effects of mass waste events on thrust wedges : Analogue experiments and application to the Makran accretionary wedge. Tectonics, 29, doi :10.1029/2009TC002526

Soto, J. I., Comas, M. C. and De La Linde, J., (1996), Espesor de sedimentos en la cuenca de Alborán mediante conversión sísmica corregida. Geogaceta 20, 382-385.

Storti, F., and McClay, K., (1995), Influence of syntectonic sedimentation on thrust wedges in analogue models. Geology 23, 999–1002, doi:10.1130 /0091-7613(1995)0232.3.CO;2

Suppe, J., (2007), Absolute fault and crustal strength from wedge tapers. Geology, 35, 1127-1130. doi: 10.1130/G24053A.1

Thurner, S., Palomeras, I., Levander, A., Carbonell, R. and Lee, C.T., (2014), Ongoing lithospheric removal in the western Mediterranean: Evidence from Ps receiver functions and thermobarometry of Neogene basalts (PICASSO project). Geochem Geophy Geosy 15, 1113-1127.Vera, J.A., (2004), Cordillera Bética y Baleares. In: Geología de España (J.A. Vera, Ed.), SGE-IGME, Madrid, 347-464.

Vera, J.A. (Eds.) (2004), Geología de España. Sociedad Geológica de España, Instituto Geológico y Minero de España.

Vergés, J., Muñoz, J. A. and Martínez, A., (1992), South Pyrenean fold-and-thrust belt: Role of foreland evaporitic levels in thrust geometry, in K. R. McClay, ed., Thrust Tectonics: London, Chapman and Hall, p. 255-264.Vitale, S., Zaghloul, M. N. and D'Assisi-Tramparulo, F., (2014), Deformation characterization of a regional thrust zone in the northern Rif (Chefchaouen, Morocco). Journal of Geodynamics 77, 22-38. doi: 10.1016/j.jog.2013.09.006

Von Hagke, C., Oncken, O. and Evseev, S., (2014), Critical taper analysis reveals lithological control of variations in detachment strength: An analysis of the Alpine basal detachment (Swiss Alps). Geochemistry, Geophysics, Geosystems 15 (1), 176-191. doi: 10.1002/2013GC005018

Woodward, N.B., (1987), Geological applicability of critical-wedge thrust-belt models. Geological Society of America Bulletin, 99, 827-832. doi: 10.1130/0016-7606(1987)99<827:GAOCTM>2.0.CO;2.

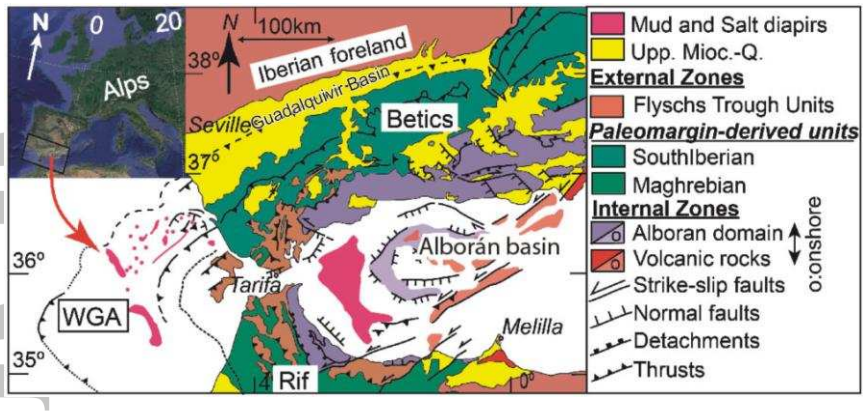

Figure 1. Location and tectonic map of the Gibraltar Arc (GA) within the Western Mediterranean; the Western GA (WGA) is a major salient

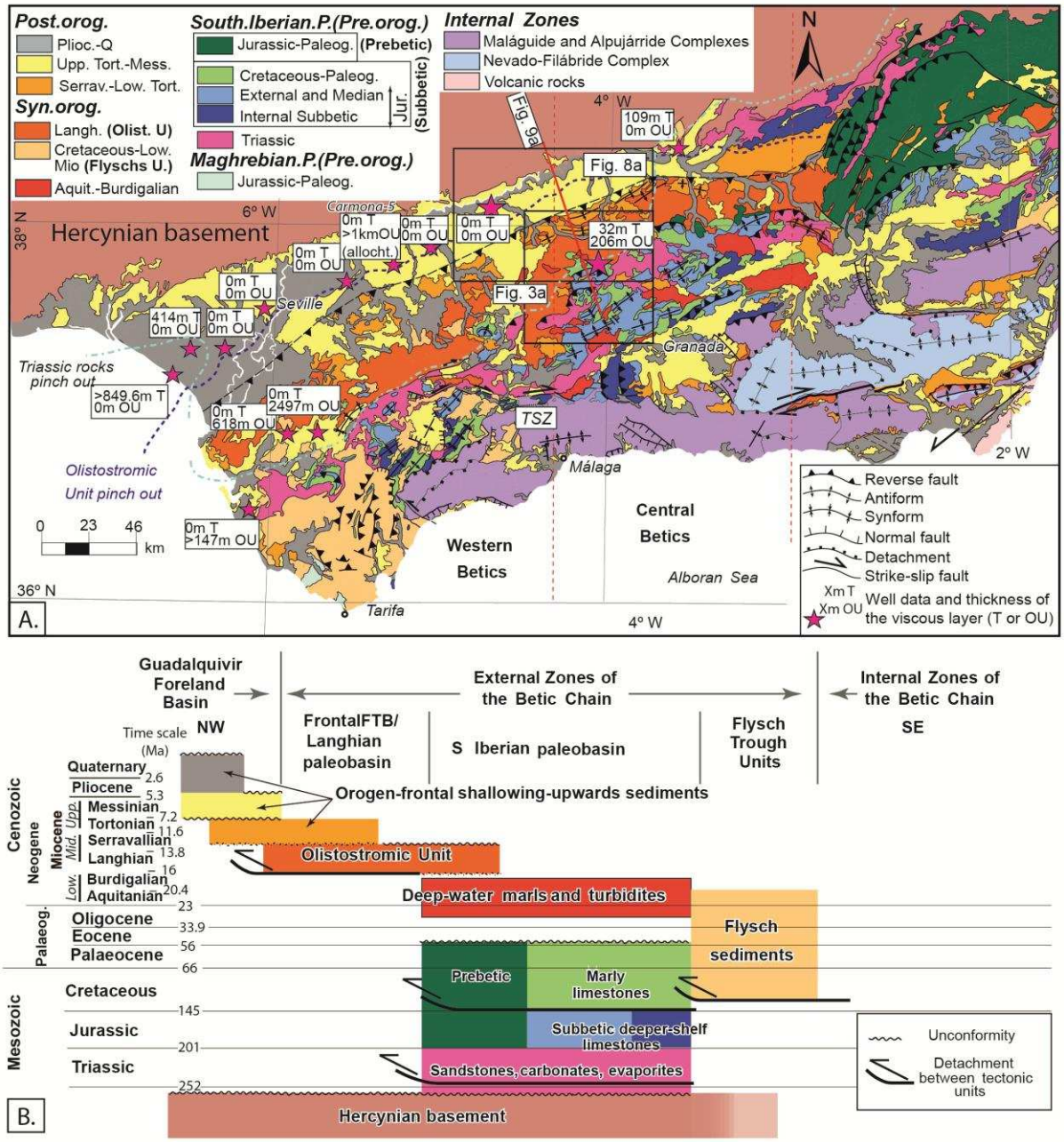

Figure 2. (a) Simplified geological map of the Betic Chain (northern branch of the Gibraltar Arc) showing the main structures (modified from Gabaldón et al., [1994]; geology based on Vera et al., [2004] and references therein). OU pinch out boundary constrained using information from Martínez del Olmo and Martín, [2016]. (b) Simplified stratigraphy and main tectonic units across the Betics (based on Vera et al., [2004]).

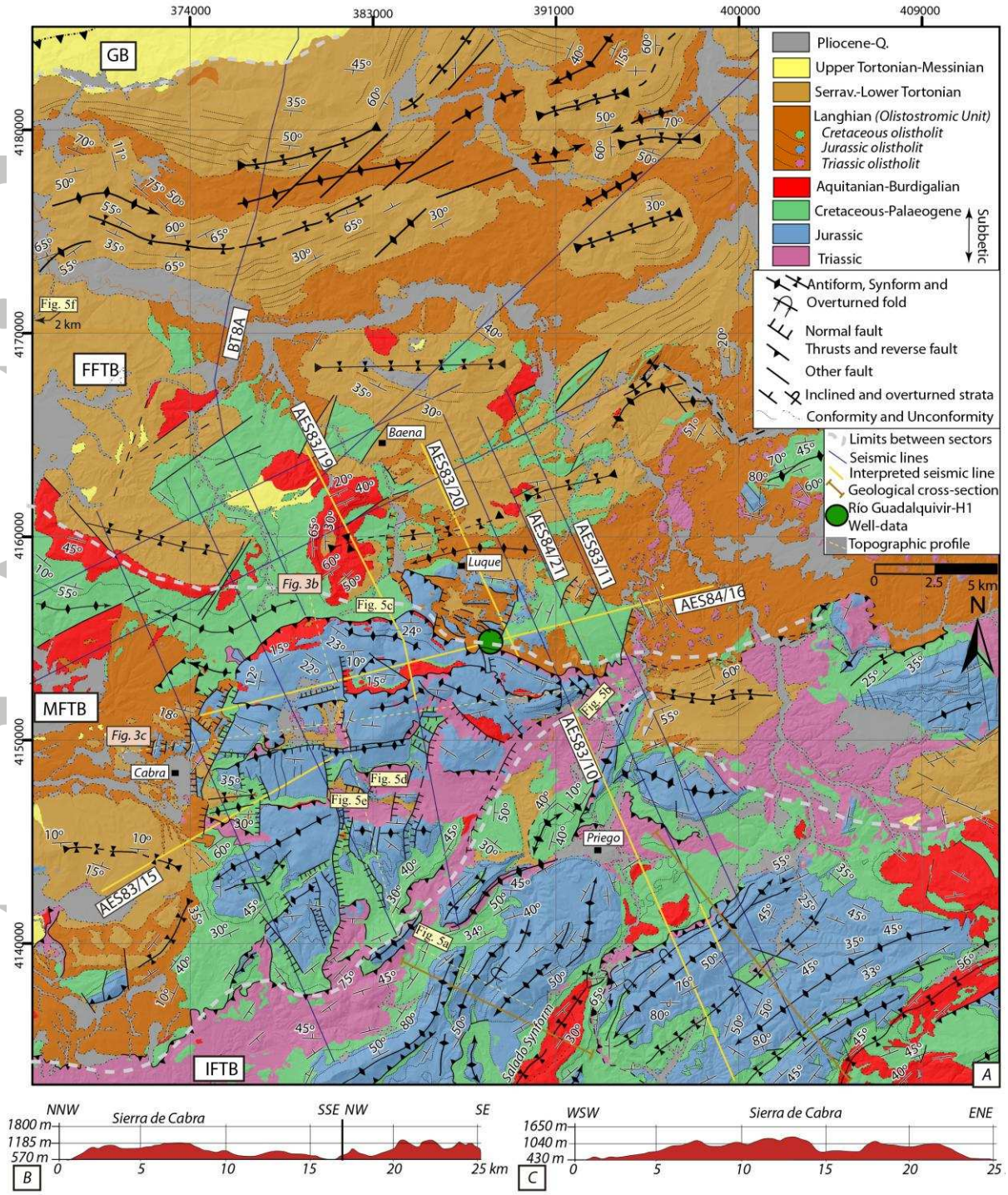

Figure 3. (a) Structural map of the studied area. The location of the well and seismic lines are indicated. (b) and (c) Representative topographic profiles along and across the orogenic strike.

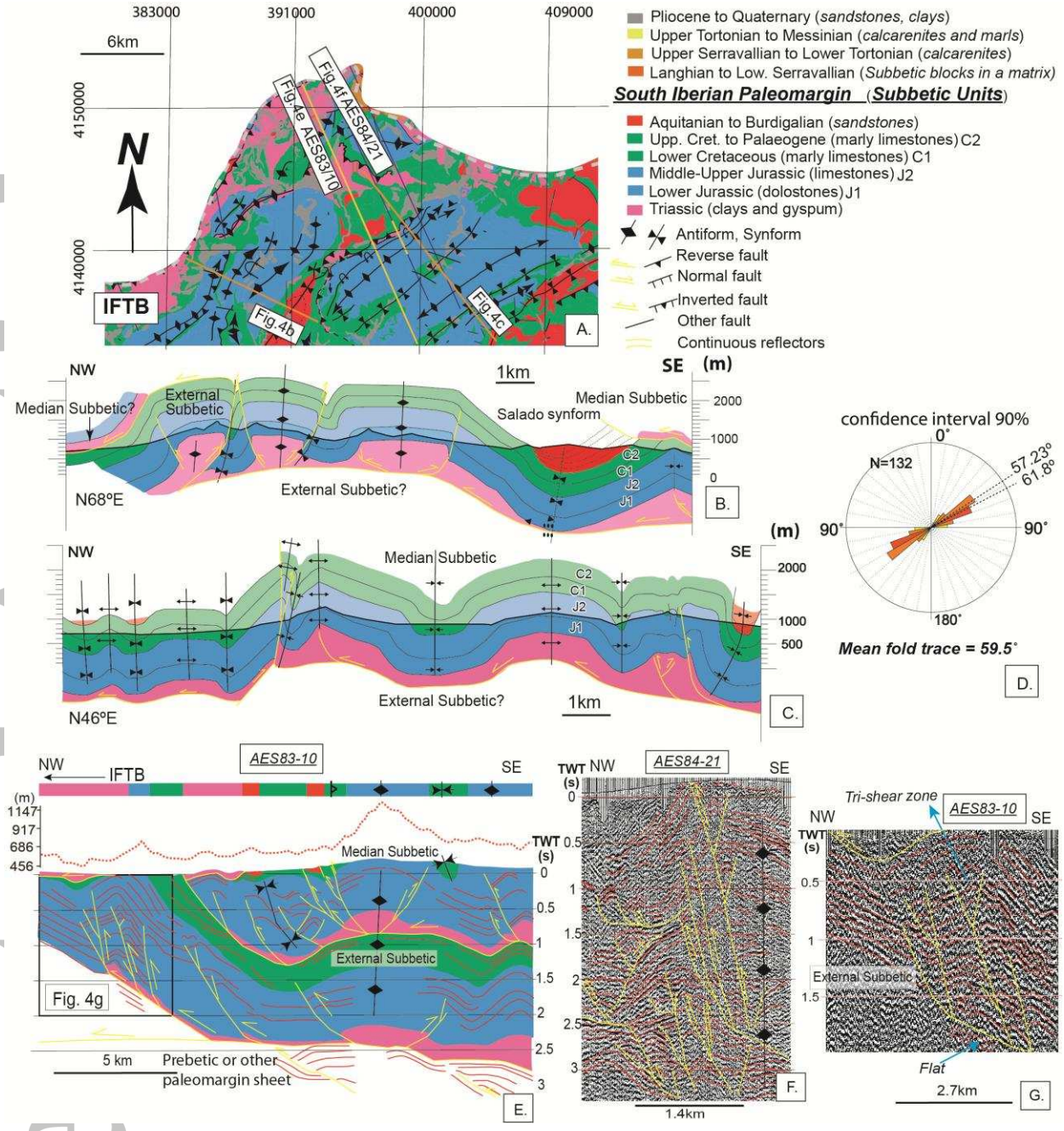

Figure 4. (a) Geological map of the IFTB. (b and c) Cross-sections subperpendicular to the fold train strike, displaying the detachment-fold geometry. (d) Rose diagram showing fold axial trace trends. (e) Interpreted seismic line parallel to the IFTB transport direction. (f) Detailed seismic interpretation of a detachment fold limb. (g) Detailed seismic interpretation of the IFTB/MFTB boundary showing a change in the thrusting style with clear NW vergences. All seismic lines are presented at rough 1:1 scale.

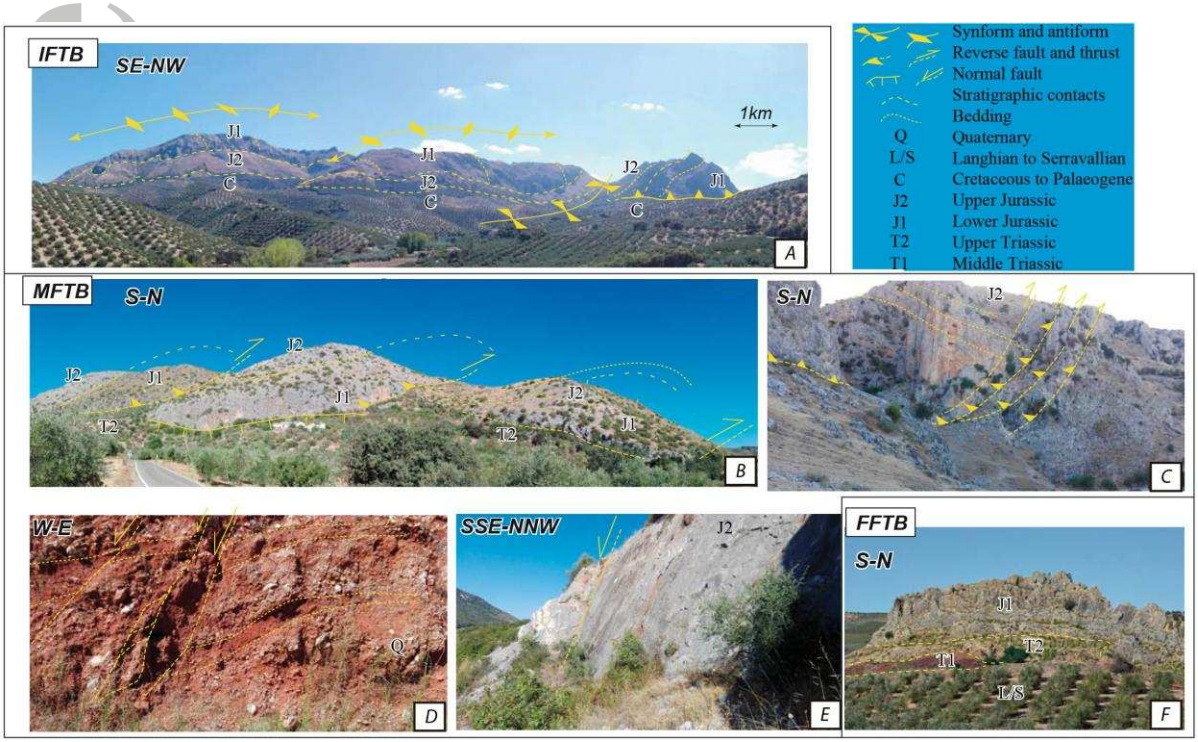

Figure 5. Photographs of representative geological features in the study area. (a) NW-SE striking folds and reverse faults of the IFTB; (b) NW-verging thrusts in the MFTB; (c) the frontal thrust scarp of the Sierra de Cabra controlling a significant relief drop; (d) Quaternary sediments in the MFTB cut by normal faults associated with arc-parallel stretching; (e) previous thrust surface reactivated as a normal fault; (f) Langhian-Serravallian matrix wrapping a Subbetic olistolith.

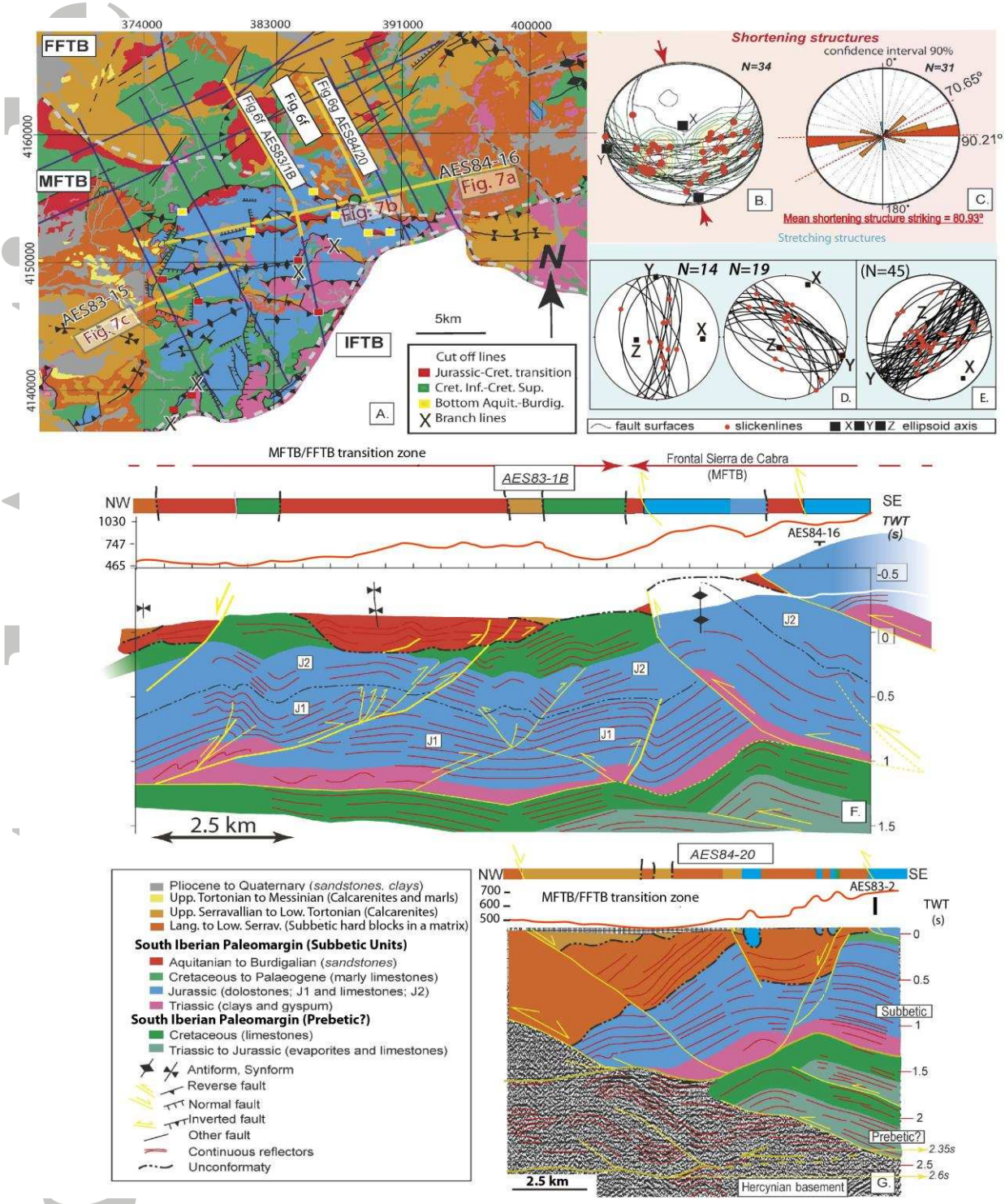

Figure 6. (a) Geological map of the MFTB. (b and c) Stereoplot and a rose diagram showing the orientation of the main shortening structures (fold axial traces and thrust strikes). (d and e) Stereoplots of the N-S, NW-SE and WSW-ENE normal faults with the approximate

orientation of the x, y and z stress axes of the ellipsoid. (f) Seismic interpretation of AES-831B correlated with lithological surface data (color bar); (g) Seismic interpretation of AES84-20 with lithological surface data (color bar) showing the deformation at the MFTB/FFTB boundary.

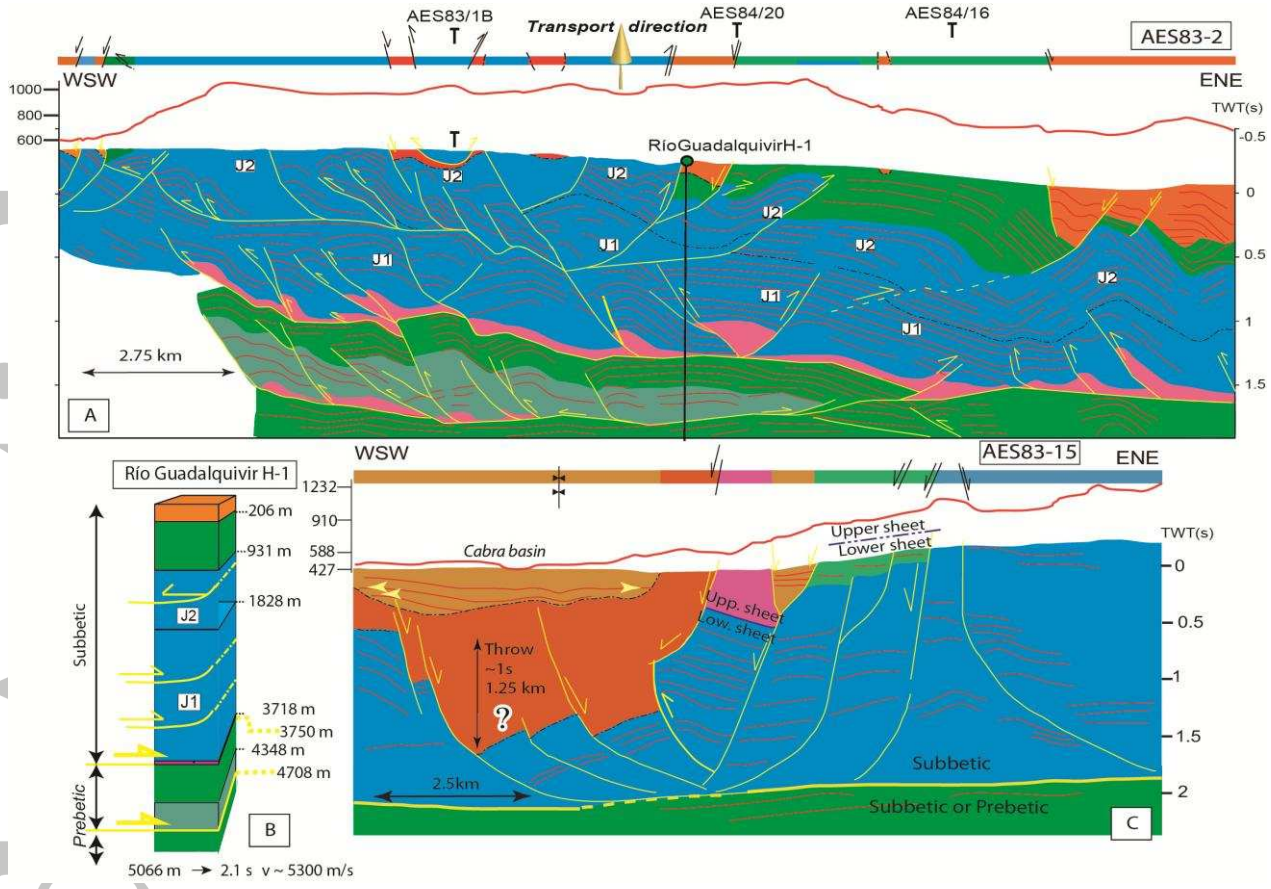

Figure 7. (a) Seismic interpretation of AES84-16 with lithological surface data (color bar) and well data. This seismic line is perpendicular to the transport direction and shows multiple lateral ramps, and normal faults caused by arc-parallel stretching. (b) Well lithological column and estimations of the average P-wave velocity (well bottom at 2.1s TWT from 0.3s above datum). (c) Seismic interpretation of AES83-15 at the W end of the Sierra de Cabra, showing the structure of the Cabra Basin.

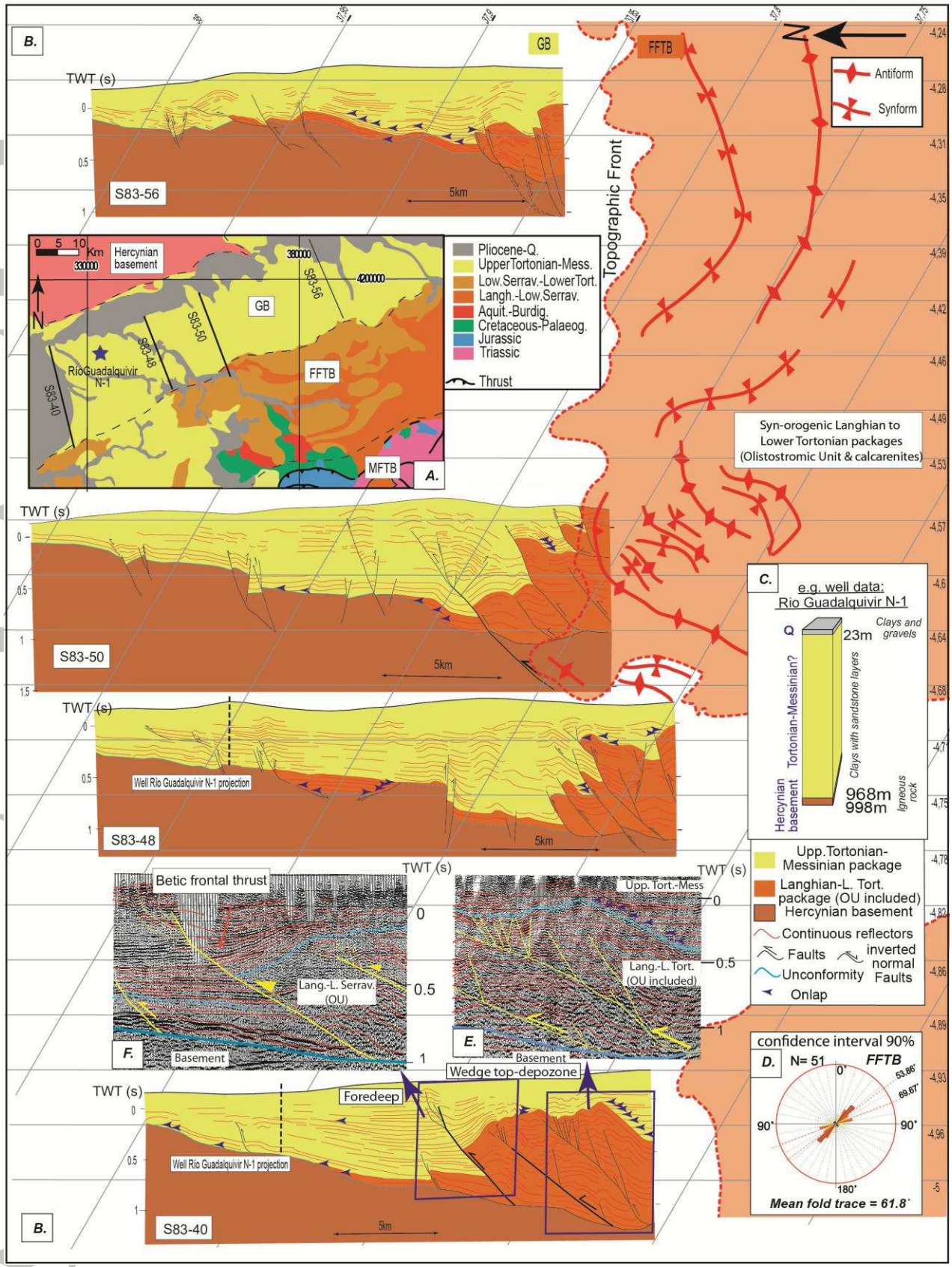

Figure 8. (a) Geological map of the FFTB and GB, and the location of the analysed seismic lines and the well Río Guadalquivir N-1 (b, c, f and e). (b) Fold axial traces within the FFTB and seismic interpretations. (c) Well Río Guadalquivir N-1 lithological column. P-wave velocity is estimated to 2500 m/s (well bottom at 0.6s TWT from 0.13s above datum). (d) Rose diagram showing the fold axial trace direction. (e) Detailed seismic profiles interpretation of the Betic frontal thrust and (f) the geometry of the fault-propagation folds in the GB.

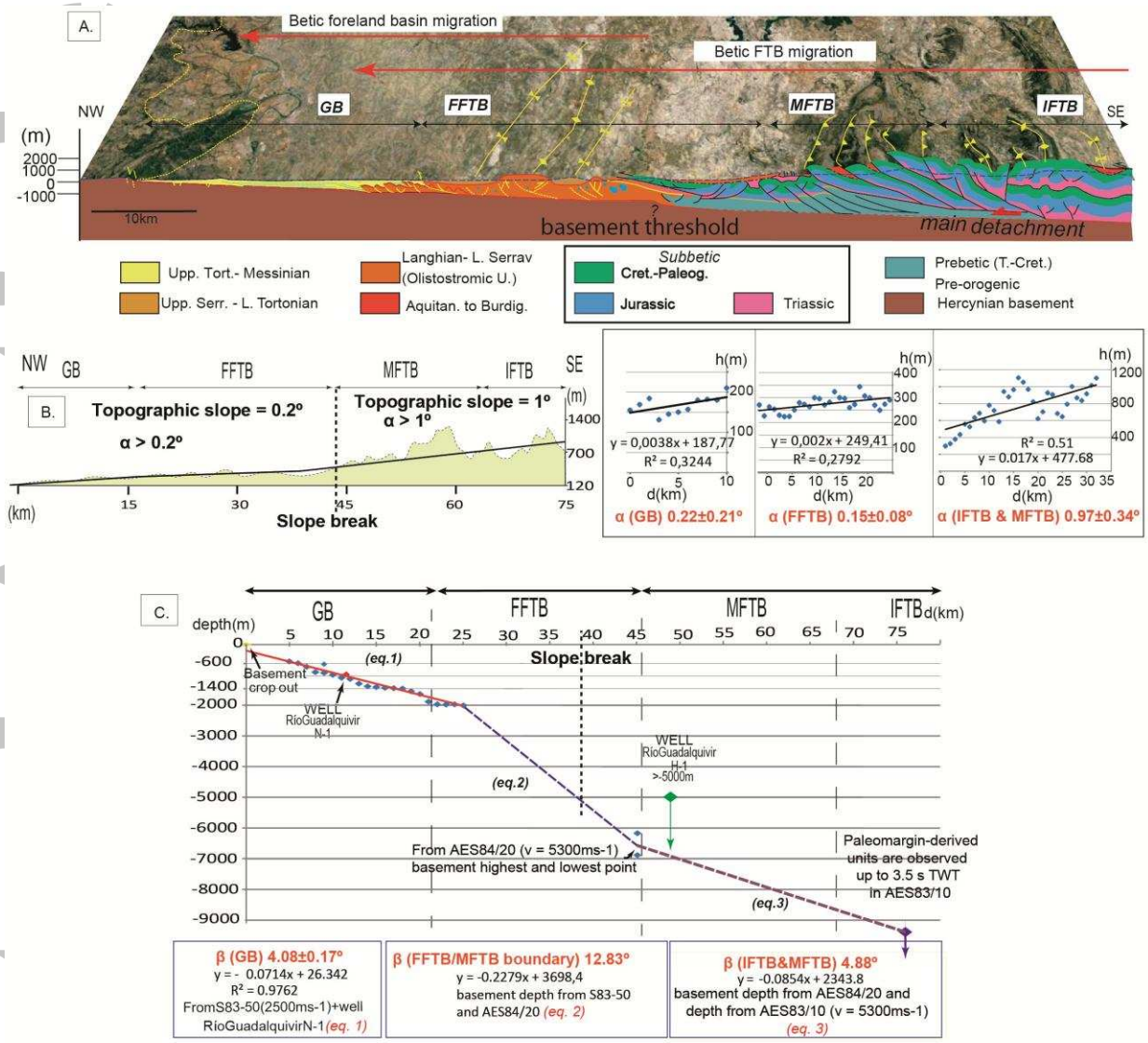

Figure 9. (a) 3D block diagram covering the studied sector and illustrating the spatial relationships of the wedge structures, the topography, and the FTB/basin migration. (b) Representative topographic profile (Location in Fig. 2a) and the topographic relief envelope α (black line). Examples of the linear regression used to calculate α in different sectors are also shown. (c) Basal slope β changes across the study area, based on seismic interpretations and well data. β steepening within the FFTB is not directly observed but a minimum β of ~12° is suggested to explain the different basement levels below the GB and the MFTB/IFTB.

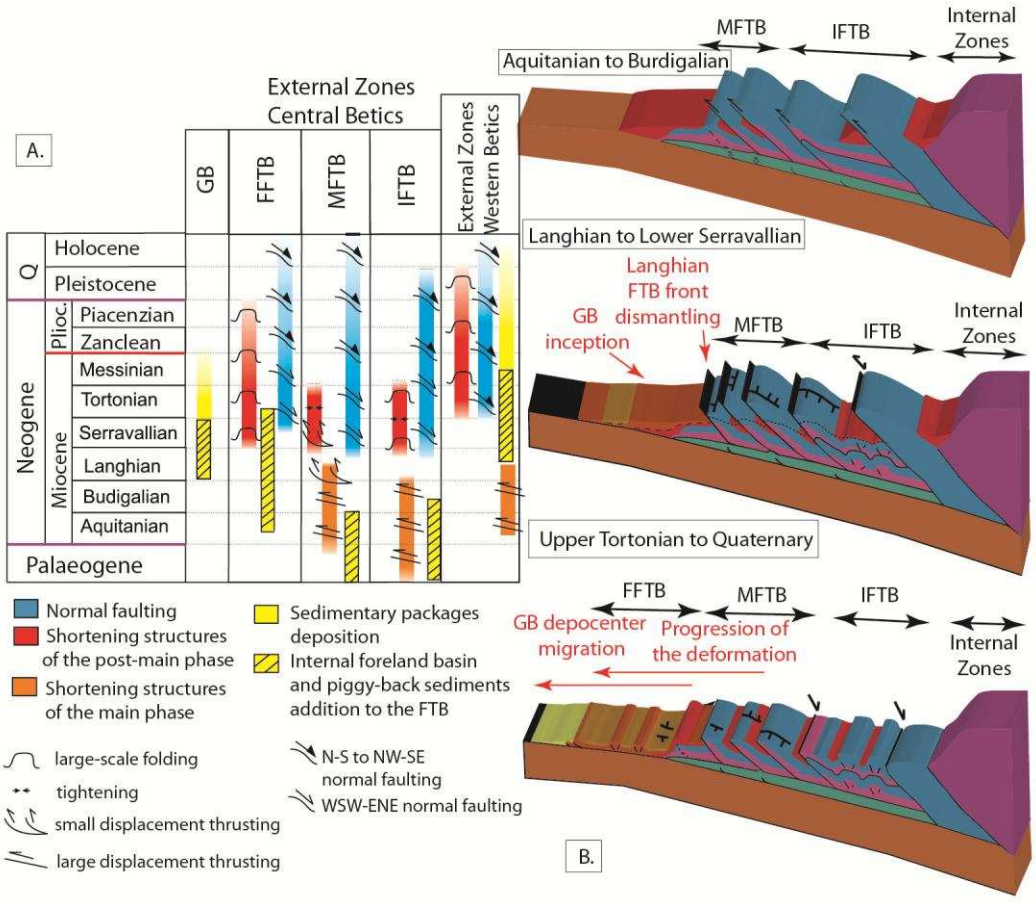

Figure 10. (a) Chronologic chart of the deformation phases of the Central Betics FTB compared with the phases in the Western Betics [Jiménez-Bonilla et al., 2015a]. (b) Schematic 3D block diagrams illustrating the evolution of the External orogenic wedge.

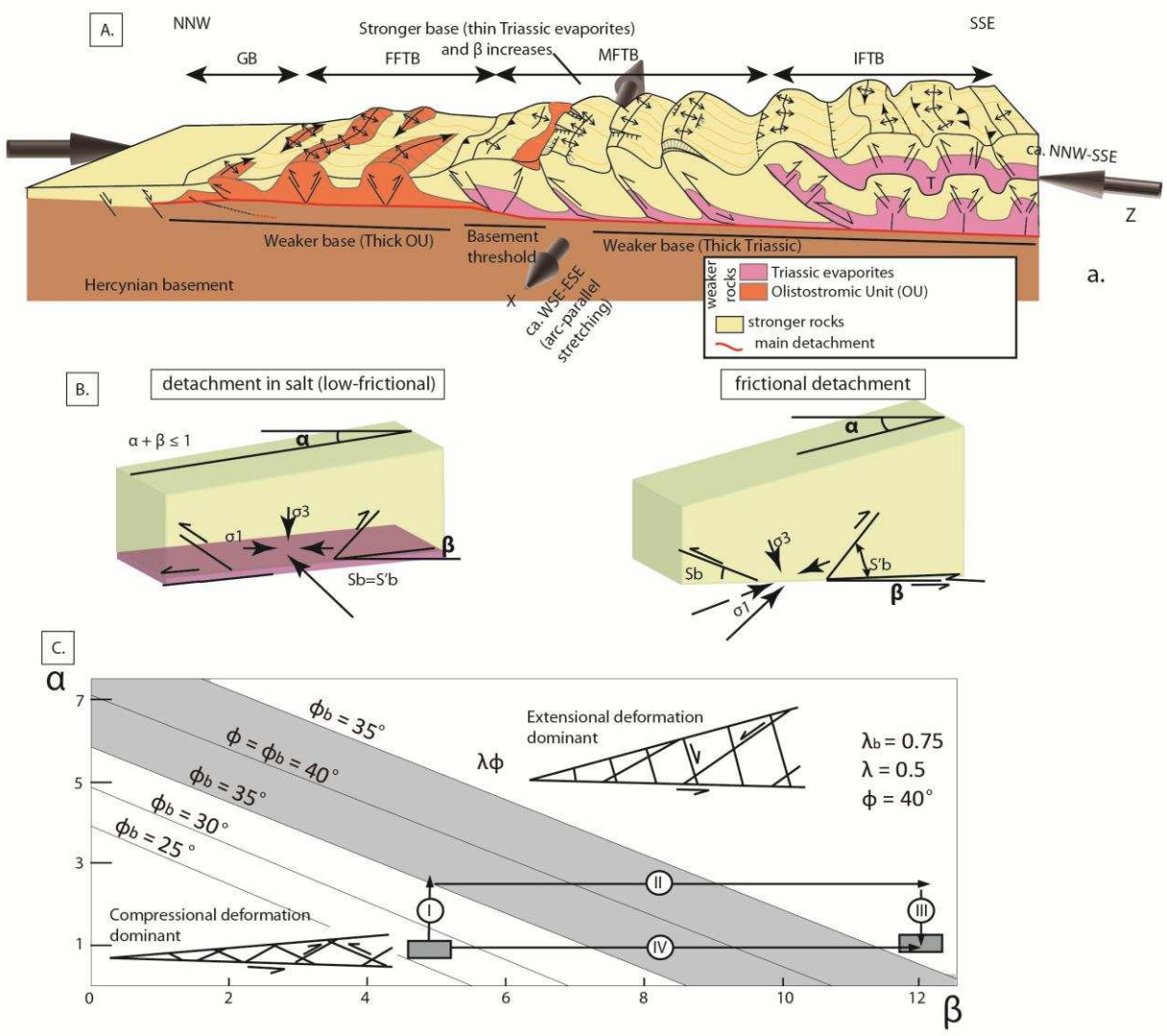

Figure 11. (a) Schematic diagram illustrating the tectonic model where the variations of β and detachment strength are correlated with the different structural styles. (b) Schematic diagrams illustrating the effect of frictional vs. non-frictional detachments on wedge geometry. (c) A simple wedge stability analysis accounting for the changes in Φ_b and β beneath IFTB/MFTB and MFTB/FFTB threshold. The approximate stability field when Φ_b=35° is shaded with grey. The graph illustrates the two scenarios as discussed in the text: 1) growth of the taper, FTB migration to the basement threshold (β=12°), resulting in the orogen-frontal collapse (I-III); 2) the frontal FTB encounters the basement threshold before/simultaneously with encountering the Triassic pinch-out (IV). Illustrations of wedge faulting styles outside the wedge stability field are adopted from Dahlen [1984].